AR-008-408

DSTO-RR-0005

Stress Intensity Factors and Crack Mouth Openings for Bridged Cracks Emanating from Circular Holes

C.R. Pickthall

DEPARTMENT OF DEFENCE

DEFENCE SCIENCE AND TECHNOLOGY ORGANISATION

Stress Intensity Factors and Crack Mouth Openings for Bridged Cracks Emanating from Circular Holes

C.R. Pickthall

Airframes and Engines Division
Aeronautical and Maritime Research Laboratory

DSTO-RR-0005

ABSTRACT

Muskhelishvili's method of complex potentials has been applied to the problems of one crack, and two diametrically opposed (symmetrical) cracks emanating from a circular hole of radius R, subjected to a biaxial load. The cracks of length a, are orthogonal to the principal applied stress σ_{yy}^{∞}, with transverse stress $\sigma_{xx}^{\infty} = \lambda\sigma_{yy}^{\infty}$. This work extends previous work through the inclusion of linear springs with spring constant k bridging the crack opening. Analysis focussed on the (normalized) design parameters of crack tip stress intensity factor F_n and crack mouth opening V_n. Their dependencies on biaxiality λ, normalized spring stiffness ka, and the geometry specified by $a_n = a/(a + R)$, were investigated. Interpolation formulae with parameters depending on a_n were fitted to the high and low ka limits of F_n and V_n. These provided a simple means for calculating F_n and V_n, in most cases to within a few percent of the numerically calculated values. An interesting comparison of the symmetrically cracked hole to the partially bridged centre crack, showed that the latter had a lower stress intensity factor in all but the very short crack cases.

Approved for Public Release

DEPARTMENT OF DEFENCE

DEFENCE SCIENCE AND TECHNOLOGY ORGANISATION

Published by

DSTO Aeronautical and Maritime Research Laboratory
GPO Box 4331
Melbourne Victoria 3001 Australia

Telephone: (03) 626 7000
Fax: (03) 626 7999

AR No. 008-408
JULY 1994

Stress Intensity Factors and Crack Mouth Openings for Bridged Cracks Emanating from Circular Holes

EXECUTIVE SUMMARY

A frequently occurring maintenance problem is the repair of fatigue cracks originating from holes in structures. One method of repair involves bonding a composite material patch over the crack, however, the effectiveness and durability of the repair must be assessed prior to application.

In this work, Muskhelishvili's mathematical method is used to model one crack, and two diametrically opposed symmetrical cracks, of length a emanating from a hole of radius R in a large thin plate. The patch is modelled by springs of stiffness k acting between the crack faces to oppose opening. This single parameter incorporates the moduli and thicknesses of the patch, adhesive and plate. The output parameters crack tip stress intensity factor (F_n) and crack mouth opening (V_n), indicate the effectiveness and durability respectively of a proposed patch repair. These parameters are tabulated, and simple interpolation formulae provided as functions of the hole relative to crack size, spring stiffness, and biaxiality of the load applied to the plate.

Author

C.R. Pickthall
Airframes and Engines Division

Colin Pickthall completed his B.Sc (Hons) in physics at Monash University in 1985, and was awarded his Ph.D. for "A Pseudopotential Investigation of Indium Thallium" in December 1993, also at Monash.

He commenced work at the Aeronautical Research Laboratory (now Aeronautical and Maritime Research Laboratory) in May 1991, undertaking mathematical modelling related to the repair of fatigue cracks in aircraft skins.

Contents

List of Tables

List of Figures

1 INTRODUCTION

Cracks in structures frequently originate from stress concentrators such as bolt holes, rather than straight edges or from centres of panels. Stress analyses for these last two cases are presented by Tada *et al.*, 1985 for a large variety of loading geometries and specimen geometries. Some results for cracks emanating from circular holes are also presented, but they are not so extensive and contain no information on the crack opening profile. They also do not include springs bridging the crack faces.

The present work was undertaken to extend the Tada *et al.*, 1985 data by including crack opening information. It also treats the case where crack opening is opposed by linear springs between the crack faces as shown in fig. 1. It is an analogous development to the work of Rose, 1987 for centre cracks and comparison with that work leads to some interesting results.

The two geometries considered here for cracks emanating from a circular hole in an infinite plate are shown in fig. 1 as (a) a single crack, and (b) two cracks emanating symmetrically on opposite sides of the hole. Two more cases were examined as

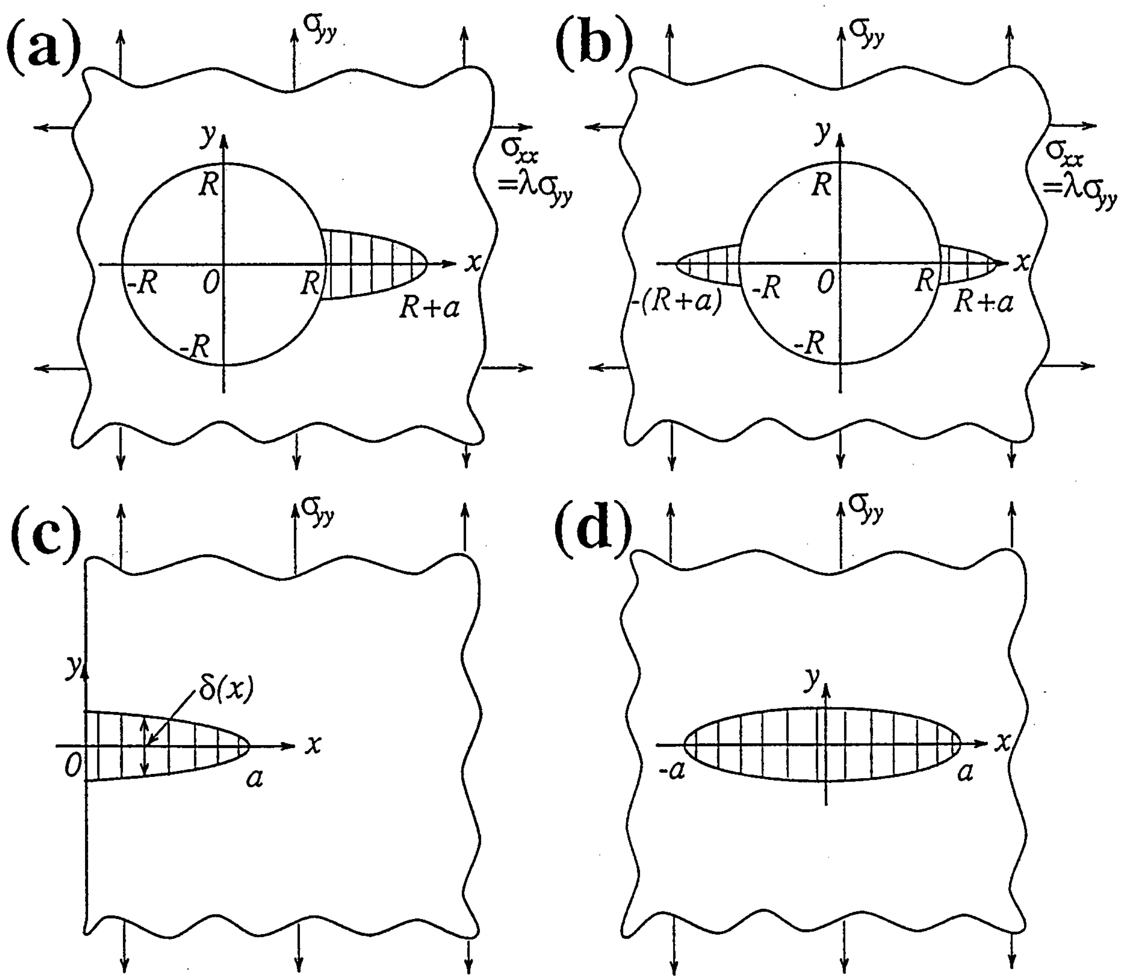

Figure 1: The loading geometry and (a) a single crack emanating from a hole, (b) the symmetric double crack case, (c) the edge crack and (d) the centre crack.

limiting behaviours of these: **(c)** an edge crack representing the large hole or short crack behaviour, and **(d)** a centre crack in an infinite plate as the small hole or long crack limit.

Loading followed the Tada *et al.*, 1985 convention where uniform remote uniaxial tension perpendicular to the crack is obtained for $\lambda = 0$, whilst $\lambda = 1$ gives biaxial loading. The presence of the hole causes the remote transverse stress σ_{xx}^{∞} to affect the behaviour, unlike the edge or centre crack cases which are insensitive to this stress.

The springs may serve to model the effect of a (repair) patch applied over the crack, leaving the hole clear, or fibre-bridging for a hole in a composite material. Stress-free boundary conditions were assumed for the hole surfaces, so that the hole may not, for example, contain an interference-fit shaft, rivet or other device that applies stresses to the hole surfaces. The general approach could, however, be extended to these cases by the introduction of appropriate boundary conditions.

The complex potential theory of Muskhelishvili, 1953 is applied in the next section to obtain the appropriate potentials for an infinite plate with a circular hole, loaded in uniform uniaxial or biaxial tension. A similar approach gives the potentials for dislocations inside or outside the hole. The requirement that the crack faces be stress-free, allowing for the effects of linear springs acting between the faces, leads to an integral equation for the distribution of dislocations which may be considered to comprise the crack.

Numerical solution of the integral equation gives the dislocation density, from which the crack opening profile, and the two important parameters K_{tip} and crack mouth opening are obtained.

Asymptotic limits for K_{tip}, known analytically, are presented in section 3, and serve as checks on the actual numerical results of the next section. An interpolation formula as a function of spring stiffness, depending parametrically on the loading and crack geometries, is presented next.

The following discussion on crack mouth openings has fewer asymptotic limits because the crack mouth opening depends heavily on conditions near the hole. In contrast, K_{tip} depends more on stresses near the tip, which may be remote from and thus less sensitive to, the hole. The interpolation formulae for crack mouth opening suggested by these limits proved to be unsuitable for some crack geometries because of unwanted divergences. Alternative forms for the interpolating functions thus had to be investigated.

The similarity of the symmetrically cracked hole case to the partially bridged centre crack of Rose, 1987 led to the interesting comparison in section 7. This indicated that in general, except for near-tip bridging, the partially bridged centre crack had a lower K_{tip}. The geometry producing equality of both cases was quite insensitive to the spring stiffness.

Table 1: Young's modulus and other parameters for plane strain or generalized plane stress conditions.

parameter	plane strain	plane stress
2μ	$E/(1+\nu)$	$E/(1+\nu)$
E'	$E/(1-\nu^2)$	E
κ	$3-4\nu$	$(3-\nu)/(1+\nu)$
$\kappa+1$	$4(1-\nu)$	$4/(1+\nu)$

2 THEORY

Throughout the analytical part of this work, the methods of Muskhelishvili, 1953 have been used to deduce the appropriate complex potentials Φ and Ψ, together with the associated (planar) stress and displacement fields. Cracks were introduced by expressing the crack-opening profile in terms of a dislocation density following Bilby and Eshelby, 1968:

$$\delta(x) = 2u_y(x, y \to 0^+) = \int_x^{a+R} D(t)\mathrm{d}t. \tag{2.1}$$

The crack mouth opening $\delta(R)$ will be the maximum crack opening for the double crack case (fig. 1(b)), but may not be for the single crack (fig. 1(b)) which is long relative to the hole radius.

The procedure is to firstly calculate the stresses around a hole in an infinite plate with no cracks, then add the appropriate distribution of dislocations while ensuring that the hole surfaces remain stress free, to produce a crack. This imposes the boundary condition

$$\sigma_{yy}(R \le x < R+a, y \to 0^+) \to 0 \tag{2.2}$$

and the same for σ_{xy}.

Prior to numerical solution, the resulting integral equation is supplemented by a term incorporating the effects of linear springs which provide a crack closing stress

$$\sigma_{yy}^{\mathrm{sp}}(x) = E'ku_y(x, 0^+) = \frac{1}{2}E'k\int_x^{a+R} D(t)\mathrm{d}t. \tag{2.3}$$

The appropriate modulus E' is given for plane strain and generalized plane stress (Tada *et al.*, 1985) in table 1.

2.1 The Hole

In treating a plate with a hole in it, a first approximation is to ignore the hole completely, thus obtaining the (far field) potentials for a plate loaded in a uniform remote stress state. These are

$$\begin{aligned} \Phi^\infty(x,y) &= \frac{1}{4}(\sigma_{xx}^\infty + \sigma_{yy}^\infty) + iC = \frac{\mathrm{d}}{\mathrm{d}z}\phi^\infty(z) \\ \Psi^\infty(x,y) &= \frac{-1}{2}(\sigma_{xx}^\infty - \sigma_{yy}^\infty) - i\sigma_{xy}^\infty = \frac{\mathrm{d}}{\mathrm{d}z}\psi^\infty(z) \end{aligned} \tag{2.4}$$

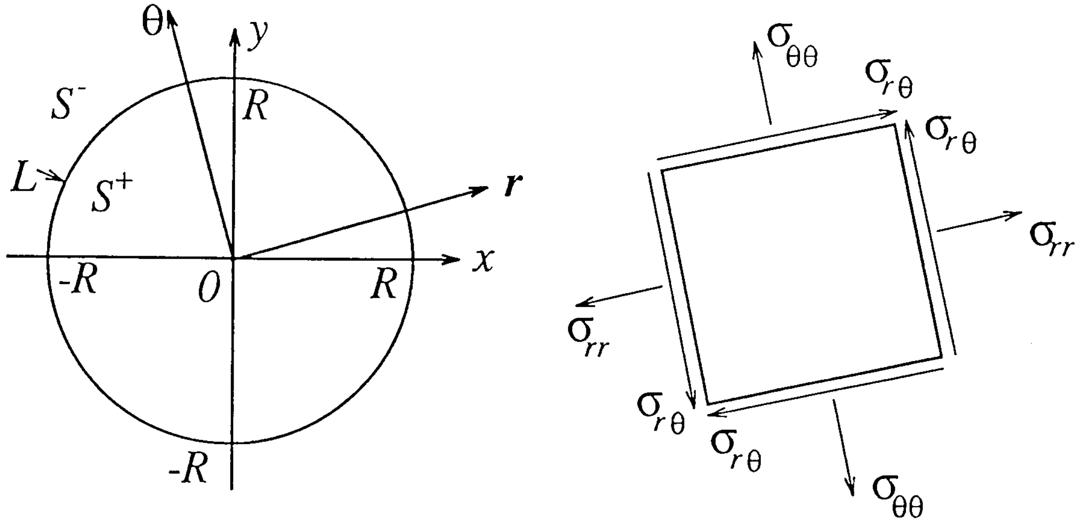

Figure 2: The regions S^+, S^- and L, together with the stresses in the rotated coordinates.

with $z = x + iy$ and C an arbitrary real constant. These may be verified by substitution into the Muskhelishvili, 1953 relations:

$$\begin{aligned} 2\mu\Big(u_x(x,y) + iu_y(x,y)\Big) &= \kappa\phi(z) - z\overline{\Phi(z)} - \overline{\psi(z)} \\ \sigma_{xx}(x,y) + \sigma_{yy}(x,y) &= 2\Big(\Phi(z) + \overline{\Phi(z)}\Big) = 4\mathrm{Re}\{\Phi(z)\} \\ \sigma_{xx}(x,y) - \sigma_{yy}(x,y) + 2i\sigma_{xy}(x,y) &= -2\Big(z\overline{\Phi'(z)} + \overline{\Psi(z)}\Big). \end{aligned} \tag{2.5}$$

Here μ denotes the shear modulus, and κ depends on Poisson's ratio ν as shown in table 1. $\Phi'(z) = \frac{\mathrm{d}\Phi}{\mathrm{d}z}$. The displacement of point (x, y) is u_x parallel to the x axis, and u_y along y. For the current problem, $C = 0$ and $\sigma_{xy}^{\infty} = 0$ in equation (2.4).

The presence of the hole modifies the potentials from (2.4) to

$$\begin{aligned} \Phi(z) &= \Phi^{\infty}(z) + \Phi^{\mathrm{h}}(z) \\ \Psi(z) &= \Psi^{\infty}(z) + \Psi^{\mathrm{h}}(z) \end{aligned} \tag{2.6}$$

where Φ^h and Ψ^h are perturbations due to the hole. They are analytic everywhere outside the hole, vanishing at infinity faster than $1/z$. This rate of decay at infinity is required to ensure that there is no net dislocation content, force or moment about the hole.

The hole surface is defined as L, points on L denoted by t, and S^+ the region inside with S^- outside the hole as shown in fig. 2. Application of the rotation of coordinates formulae

$$\begin{aligned} u_r + iu_\theta &= \exp(-i\theta)(u_x + iu_y) \\ \sigma_{rr} + \sigma_{\theta\theta} &= \sigma_{xx} + \sigma_{yy} \\ \sigma_{rr} - \sigma_{\theta\theta} + 2i\sigma_{r\theta} &= \exp(-i2\theta)(\sigma_{xx} - \sigma_{yy} + 2i\sigma_{xy}) \end{aligned} \tag{2.7}$$

to equation (2.5), together with $\exp(-i2\theta) = \overline{z}/z$, allows the stress-free hole surface boundary condition to be written

$$\sigma_{rr}(t) + i\sigma_{r\theta}(t) = 0 = \Phi(z) + \overline{\Phi(z)} - \overline{z\Phi'(z)} - (\overline{z}/z)\overline{\Psi(z)} \tag{2.8}$$

as $z \rightarrow t$ from S^-.

The idea now, is that we seek to re-express this in the form

$$0 = \Phi(z \rightarrow t^-) + \Omega(z^* \rightarrow t^+) \tag{2.9}$$

where the function $\Omega(z^*)$ need only be defined for $z^* \in S^+$ being an as yet unspecified function of $z \in S^-$. The only requirement on z^* is that, as z approaches $t \in L$ from S^+, then z^* approaches t from S^-. $\Omega(z^*)$ will be expressed in terms of $\Phi(z)$ and $\Psi(z)$ such that (2.8) is replaced by (2.9) in the $z \to t$ limit.

If this can be done, then the function $F(z)$ defined by

$$F(z) = \begin{cases} \Phi(z) & ,z \in S^- \\ -\Omega(z), & z \in S^+ \end{cases} \tag{2.10}$$

is analytic across the boundary L. Its behaviour for $z \in S^-$ is dictated by that for $\Phi^-(z)$. The behaviour at ∞, and any poles in S^- are thus specified. For the behaviour in S^+, we look at the singularities determined by the form of $\Omega(z^*)$: these may occur at $z^* \to 0$, and at points determined once more, by the known singularities in $\Phi(z)$ and $\Psi(z)$.

$F(z)$ is therefore a function analytic in the whole plane except at known poles with known coefficients, and a prescribed behaviour at ∞. It must be of the form

$$F(z) = \sum_j \sum_{n=1}^{n_j} \frac{c_{jn}}{(z - z_j)^n} + \sum_{k=0}^{N} d_k z^k. \tag{2.11}$$

This gives $\Phi(z)$ directly for $z \in S^-$, and $\Psi(z)$ may be found by inverting the expression for $\Omega(z^*)$.

In the present problem, a suitable expression is

$$\Omega(z^*) = \overline{\Phi}(R^2/z^*) - (R^2/z^*)\overline{\Phi'}(R^2/z^*) - (R^2/z^{*2})\overline{\Psi}(R^2/z^*) \tag{2.12}$$

with $z^* = R^2/\overline{z}$ as suggested by List, 1969. Equation (2.8) then becomes

$$\sigma_{rr}(z) + i\sigma_{r\theta}(z) = \Phi(z) + \Omega(R^2/\overline{z}) + \left(\frac{\overline{z}^2}{R^2} - \frac{\overline{z}}{z}\right)\overline{\Psi(z)}. \tag{2.13}$$

As $z \to t \in L$ from S^-, $(R^2/\overline{z}) \to t$ from S^+ and the last term above vanishes. The left side becomes zero due to the stress-free boundary condition (2.8). This equation reduces, on L as required, to (2.9). The analytic continuation arguments above lead to the function $F(z)$ given by (2.11), with singularities prescribed by equations (2.4), (2.6), and (2.12). From (2.6) and (2.4), $N = 0$ and $d_0 = \frac{1}{4}(\sigma_{xx}^\infty + \sigma_{yy}^\infty)$. The other singularity in $F(z)$ arises as $z \to 0$ in the last term of (2.12): $\Omega(z \to 0) \to -(R^2/z^2)\overline{\Psi}(|z| \to \infty)$. Finally,

$$F(z) = -\frac{R^2}{2z^2}(\sigma_{xx}^\infty - \sigma_{yy}^\infty) + \frac{1}{4}(\sigma_{xx}^\infty + \sigma_{yy}^\infty). \tag{2.14}$$

Equation (2.12) may be rewritten to make $\Psi(z)$ the subject:

$$\Psi(z) = (R^2/z^2)\Phi(z) - (R^2/z)\Phi'(z) - (R^2/z^2)\overline{\Omega}(R^2/z). \tag{2.15}$$

Making use of (2.11) and (2.14), and noting that if $z \in S^-$ then $R^2/z \in S^+$, we obtain both potentials as

$$\begin{aligned} \Phi^-(z) &= \sigma_{xx}^\infty\left(\frac{1}{4} - \frac{R^2}{2z^2}\right) + \sigma_{yy}^\infty\left(\frac{1}{4} + \frac{R^2}{2z^2}\right) \\ \Psi^-(z) &= \sigma_{xx}^\infty\left(\frac{-1}{2} + \frac{R^2}{2z^2} - \frac{3R^4}{2z^4}\right) + \sigma_{yy}^\infty\left(\frac{1}{2} + \frac{R^2}{2z^2} + \frac{3R^4}{2z^4}\right). \end{aligned} \tag{2.16}$$

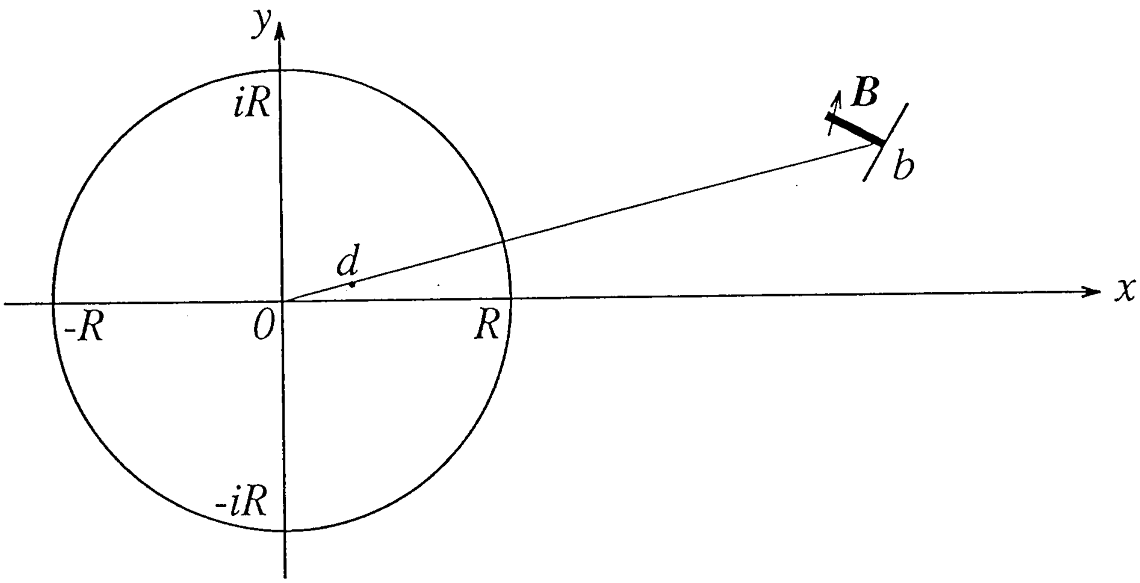

Figure 3: A dislocation of Burgers' vector $\mathbf{B} = B_x + iB_y$ located at point b outside a hole of radius R. The image point is at $d = R^2/\bar{b}$ inside the hole.

2.2 Dislocation Outside the Hole

In addition to the potentials developed in the previous section, we need the potentials for a dislocation outside the hole as in fig. 3, and also those for one inside the hole, treated in the next section. We begin with the potentials for a dislocation at the origin in an infinite plate:

$$\begin{aligned}\Phi^0(z) &= \frac{-\mu}{\pi(1+\kappa)}\frac{iB_x - B_y}{z} = \frac{-i\lambda}{z} \\ \Psi^0(z) &= \frac{\mu}{\pi(1+\kappa)}\frac{iB_x + B_y}{z} = \frac{i\bar{\lambda}}{z}\end{aligned} \tag{2.17}$$

where $\lambda = \frac{\mu}{\pi(1+\kappa)}\mathbf{B}$ and $\mathbf{B} = B_x + iB_y$ denotes the Burgers' vector. List, 1969 appears to have a sign wrong in his equation 2.7 which should have $-C = D$. The above are correct by substitution into equations (2.5). Application of the translation of coordinates formulae

$$\begin{aligned}z_B &= z_A - z_{BA} \\ \Phi_B(z_B) &= \Phi_A(z_A) \\ \Psi_B(z_B) &= \Psi_A(z_A) + \overline{z_{BA}}\Phi'_B(z_B)\end{aligned} \tag{2.18}$$

gives the potentials due to a dislocation at b as

$$\begin{aligned}\Phi^D(z) &= \frac{-i\lambda}{z-b} \\ \Psi^D(z) &= \frac{i\bar{\lambda}}{z-b} - \frac{i\lambda\bar{b}}{(z-b)^2}.\end{aligned} \tag{2.19}$$

The hole modifies these due to the stress-free hole surface in much the same way as for the remote applied stress case. Equations (2.6) to (2.11) still apply with Φ^∞ and Ψ^∞ replaced by Φ^D and Ψ^D respectively. The singularities in $F(z)$ as given by (2.11) will differ, so from there a separate treatment is required.

Singularities in Φ^D and Ψ^D produce

$$\Omega^{\text{singular}}(z) = \frac{i\overline{\lambda}}{(R^2/z)-\overline{b}} - \frac{R^2}{z}\frac{-i\overline{\lambda}}{\left((R^2/z)-\overline{b}\right)^2} - \frac{R^2}{z^2}\frac{-i\lambda}{(R^2/z)-\overline{b}} + \frac{R^2}{z^2}\frac{-i\overline{\lambda}b}{\left((R^2/z)-\overline{b}\right)^2}. \tag{2.20}$$

Using $d = R^2/\overline{b}$, expanding using partial fractions, and collecting pole-type terms, $F(z)$ becomes

$$F(z) = \frac{-i\lambda}{z-b} + \frac{i\lambda}{z-d} - \frac{i\lambda}{z} + \frac{i\overline{\lambda}d(b-d)}{\overline{b}(z-d)^2}. \tag{2.21}$$

Equation (2.15) becomes, using (2.21) in (2.11),

$$\begin{aligned}\Psi(z) \quad = \quad & \frac{-2i\lambda R^2}{z^3} + \frac{i\lambda R^2(2z-d)}{z^2(z-d)^2} - \frac{i\lambda R^2(2z-b)}{z^2(z-b)^2} \\ & + \frac{i\overline{\lambda}d^2(b-d)(3z-d)}{z^2(z-d)^3} + \frac{i\overline{\lambda}}{z} - \frac{i\overline{\lambda}d}{z(z-d)} + \frac{i\overline{\lambda}b}{z(z-b)} - \frac{i\lambda(\overline{b}-\overline{d})}{(z-b)^2}.\end{aligned} \tag{2.22}$$

This may be simplified by partial fractions, producing

$$\begin{aligned}\Psi(z) \quad = \quad & \frac{i\overline{\lambda}}{z-b} - \frac{i\lambda\overline{b}}{(z-b)^2} - \frac{i\overline{\lambda}}{z-d} + \frac{i\overline{\lambda}}{z} - \frac{2i\lambda R^2}{z^3} \\ & + \frac{i}{z^2}\left(\overline{\lambda}(b-d) - \lambda(\overline{b}-\overline{d})\right) + \frac{i}{(z-d)^2}\left(\lambda\overline{b} - \overline{\lambda}(b-d)\right) \\ & + \frac{2i\overline{\lambda}d(b-d)}{(z-d)^3}.\end{aligned} \tag{2.23}$$

2.3 Dislocation Inside the Hole

The potentials are now sought for a dislocation located inside the hole, for convenience at the origin. These are then combined with those from the previous section to render no net dislocation content far from the hole. The procedure is the same as before, but Φ^D and Ψ^D are replaced by Φ^0 and Ψ^0 from equation (2.17). The only singularity in $F(z)$ by (2.11) is as $z \to 0$ in the $\Omega(z)$ term: $\Omega(z \to 0) \to \frac{i\lambda}{z}$. This is from the $-(R^2/z^2)\overline{\Psi}(R^2/z)$ term. Equation (2.21) is replaced by

$$F^0(z) = \frac{-i\lambda}{z} = \Phi^0(z), \tag{2.24}$$

and substitution into (2.15) produces

$$\Psi^{0\text{h}}(z) = \frac{i\overline{\lambda}}{z} - \frac{2i\lambda R^2}{z^3}. \tag{2.25}$$

This has been superscripted "0h" to distinguish it from Ψ^0 in equation (2.17).

2.4 Stresses Along $y = 0$

Knowing the potentials for all three cases, the stresses $\sigma_{yy}(x, y = 0)$ they produce need to be calculated. These stresses enter into the crack-defining condition (2.2) and produce the integral equation for the dislocation density and hence crack profile.

We put $z = x$ in (2.16), (2.21), and (2.23) to (2.25), and substitute these into (2.5) to obtain $\sigma_{yy}(x,0)$. Furthermore, b is taken to be real so that $d = R^2/b$ is also real, and $\lambda = iB_n$, that is Burgers' vector is purely imaginary (iB_y only). These simplifications make $\Phi(x)$ and $\Psi(x)$ real, where the $y = 0$ has been omitted for brevity. Equations (2.5) indicate that $\sigma_{xy}(x) \equiv 0$ as required, and

$$\sigma_{yy}(x) = 2\Phi(x) + x\Phi'(x) + \Psi(x). \tag{2.26}$$

Using this equation and the above simplifications, the following results are obtained where $B_n = \frac{\mu B_y}{\pi(1+\kappa)}$.

1. Uniform remote (biaxial) tension:

$$\begin{aligned}\sigma_{yy}(x \geq R) &= \sigma_{yy}^{\infty}\left(1 + \frac{1}{2}(R/x)^2 + \frac{3}{2}(R/x)^4\right) \\ &\quad + \sigma_{xx}^{\infty}\left(\frac{1}{2}(R/x)^2 - \frac{3}{2}(R/x)^4\right).\end{aligned} \tag{2.27}$$

2. Dislocation located at (real) $b > R$:

$$\begin{aligned}\sigma_{yy}(x \geq R) &= 2B_n\left\{\frac{1}{x-b} + \frac{1}{x} - \frac{1}{x-d} + \frac{b-d}{x^2} + \frac{R^2}{x^3}\right. \\ &\quad \left. + \frac{d-b}{(x-d)^2} - \frac{d\big(d-b+d(1-d/b)\big)}{(x-d)^3}\right\}.\end{aligned} \tag{2.28}$$

3. Dislocation with Burgers' vector $\mathbf{B}' = iB'_y$ with $B'_n = \frac{\mu B'_y}{\pi(1+\kappa)}$ located at $b = 0$ inside the hole:

$$\sigma_{yy}(x \geq R) = 2B'_n\left(\frac{1}{x} + \frac{R^2}{x^3}\right). \tag{2.29}$$

   Burgers' vector is dashed here to distinguish it from the previous item: later we will set $B'_n = -B_n$.

4. Putting $R \to 0$ implies $d \to 0$ and only the first term remains in equation (2.28). This is the stress due to a dislocation at b in an infinite plate.

$$\sigma_{yy}(x) = \frac{2B_n}{x-b} \tag{2.30}$$

   which could equally well have been derived directly from equations (2.26) and (2.19).

5. The other limiting case occurs as $R \to \infty$, when the situation becomes a dislocation located at b from an edge at $x = 0$. This is shown in fig. 4, and treated in the next section.

2.5 Dislocation Near an Edge

The potentials for a dislocation near an edge, as shown in fig. 4, may be derived in a similar procedure to that for the hole case. The free-boundary condition still

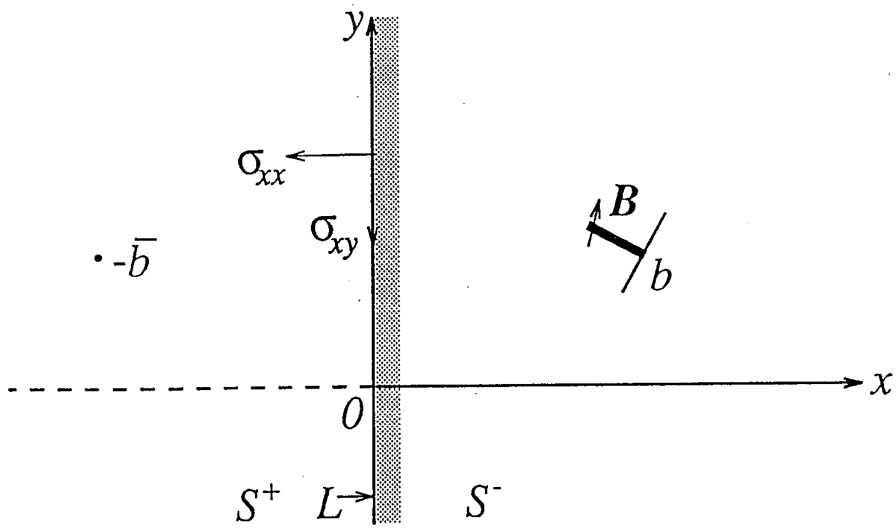

Figure 4: A dislocation of Burgers' vector $\mathbf{B} = B_x + iB_y$ located at point b in a body occupying region S^- with its edge L along $x = 0$. Along the edge, the boundary condition is $\sigma_{xx} + i\sigma_{xy} = 0$. An image dislocation is located in S^+ at $-\bar{b}$.

applies, but now to the edge rather than the hole surface of the previous case. From equations (2.5), with the edge along $x = 0$,

$$\begin{aligned} \sigma_{xx}(x,y) + i\sigma_{xy}(x,y) &= \Phi(z) + \overline{\Phi(z)} - z\overline{\Phi'(z)} - \overline{\Psi(z)} \\ &\rightarrow 0 \quad \text{as } x \rightarrow 0^+. \end{aligned} \tag{2.31}$$

For the edge case, equation (2.12) is replaced by

$$\Omega(z \in S^+) = \overline{\Phi}(-z) - z\overline{\Phi'}(-z) - \overline{\Psi}(-z) \tag{2.32}$$

so that

$$\sigma_{xx}(x,y) + i\sigma_{xy}(x,y) = \Phi(z) + \Omega(-\bar{z}) - (z + \bar{z})\overline{\Phi'}(z). \tag{2.33}$$

As $z \rightarrow t \in L$, $\sigma_{xx} + i\sigma_{xy}$ must vanish, and $\bar{z} \rightarrow -z$ as z becomes purely imaginary, so that once again, $\Phi^-(t) + \Omega^+(t) = 0$. Using the same analytic continuation arguments as before, and noting the prescribed singularities from equations (2.19) and (2.32), we obtain $F(z)$ as

$$F(z) = \frac{-i\lambda}{z-b} + \frac{i\lambda}{z+\bar{b}} + \frac{i\bar{\lambda}(b+\bar{b})}{(z+\bar{b})^2}. \tag{2.34}$$

Equation (2.32) may be rewritten as

$$\Psi(z) = \Phi(z) + z\Phi'(z) - \overline{\Omega}(-z), \tag{2.35}$$

from which

$$\Psi(z) = \frac{i\bar{\lambda}}{z-b} - \frac{i\lambda\bar{b}}{(z-b)^2} - \frac{i\bar{\lambda}}{z+\bar{b}} + \frac{i\lambda\bar{b}}{(z+\bar{b})^2} - \frac{i\bar{\lambda}(b+\bar{b})}{(z+\bar{b})^2} + \frac{2i\overline{\lambda b}(b+\bar{b})}{(z+\bar{b})^3}. \tag{2.36}$$

These potentials, with the same simplifying assumptions as before, produce σ_{yy} stresses, on the positive real axis, of

$$\begin{aligned} \sigma_{yy}(x) &= 2B_n\left(\frac{1}{x-b} - \frac{1}{x+b} - \frac{2b}{(x+b)^2} + \frac{4b^2}{(x+b)^3}\right) \\ &= 2B_n\frac{8b^2x}{(x-b)(x+b)^3}. \end{aligned} \tag{2.37}$$

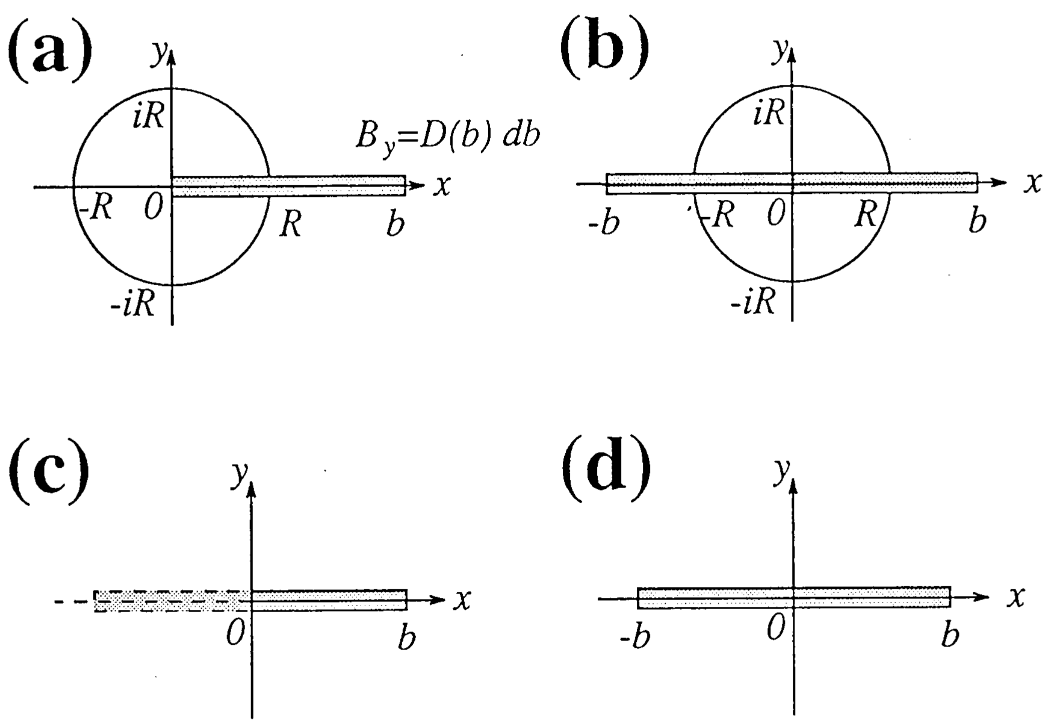

Figure 5: Crack elements used for the cases of fig. 1. In each case except the edge (c), the element actually consists of the superposition of two dislocations and the stresses they produce.

2.6 Integral Equation for the Dislocation Density

The crack opening profile is now calculated by representing the crack as a distribution of dislocations along the x axis according to equation (2.1). The stress $\sigma_{yy}(x)$ is then equal to the sum of all the stresses caused by these dislocations, that due to the (remote) applied load, and the term (2.3) due to the bridging springs. This total must be zero for each x within the crack, as the crack surfaces are stress-free according to (2.2).

The form of the dislocation density depends on the geometry of the problem being solved. For the cases (except the edge crack) being examined here, it is simpler to take the crack elements as dislocation pairs as shown in fig. 5 rather than individual dislocations. This permits automatic satisfaction of the no net dislocation content and symmetry constraints.

Taking the single crack from a hole case (a) in fig. 5, the crack element causes a stress for $R \leq x \leq R+a$ given by equation (2.28) minus (2.29) with $B_n = \frac{\mu}{\pi(1+\kappa)} D(b)\mathrm{d}b = B_n'$. The total stress at x due to the crack is then the integral of this with respect to b:

$$\begin{aligned}\sigma_{yy}^{\mathrm{h1}}(x) &= \frac{2\mu}{\pi(1+\kappa)} \int_R^{R+a} \left(\frac{1}{x-b} - \frac{1}{x-d} + \frac{b-d}{x^2} + \frac{d-b}{(x-d)^2} \right. \\ &\quad \left. - \frac{d\big(d-b+d(1-d/b)\big)}{(x-d)^3} \right) D(b)\mathrm{d}b \end{aligned} \qquad (2.38)$$

where $d = R^2/b$.

The integral equation for the dislocation density then results by combining this, the term due to springs (2.3) and that due to the applied load (2.27) in (2.2):

$$\begin{aligned}\sigma_{yy}^{\mathrm{tot}}(x) = 0 &= \frac{2\mu}{\pi(1+\kappa)}\int_R^{R+a} f(x,b;R)D(b)\mathrm{d}b - \frac{1}{2}E'k\int_x^{R+a} D(b)\mathrm{d}b \\ &+\sigma_{yy}^{\infty}\left(1+\frac{1}{2}(R/x)^2+\frac{3}{2}(R/x)^4\right)+\sigma_{xx}^{\infty}\left(\frac{1}{2}(R/x)^2-\frac{3}{2}(R/x)^4\right).\end{aligned} \tag{2.39}$$

For the single crack from a hole, $f(x,b;R)$ is

$$F^{\mathrm{h1}}(x,b;R) = \frac{1}{x-b} - \frac{1}{x-d} + \frac{b-d}{x^2} + \frac{d-b}{(x-d)^2} - \frac{d\big(d-b+d(1-d/b)\big)}{(x-d)^3} \tag{2.40}$$

whilst for the symmetric double crack it is obtained from (2.28) and the same subtracted after replacing b and d by $-b$ and $-d$ respectively:

$$\begin{aligned}F^{\mathrm{h2}}(x,b;R) &= \frac{1}{x-b} - \frac{1}{x+b} - \frac{1}{x-d} + \frac{1}{x+d} + \frac{2(b-d)}{x^2} \\ &+(d-b)\left(\frac{1}{(x-d)^2}+\frac{1}{(x+d)^2}\right) \\ &-d\big(d-b+d(1-d/b)\big)\left(\frac{1}{(x-d)^3}-\frac{1}{(x+d)^3}\right).\end{aligned} \tag{2.41}$$

The centre and edge crack cases are obtained by setting $R = 0$ in (2.39), reducing the remote loading term to σ_{yy}^{∞}. The integration ranges become 0 to a and x to a. $f(x,b;R)$ becomes a function of (x,b) only, obtained from (2.37) as

$$f(x,b) = \frac{8b^2x}{(x-b)(x+b)^3} \tag{2.42}$$

for an edge crack, and

$$f(x,b) = \frac{1}{x-b} - \frac{1}{x+b} \tag{2.43}$$

from (2.30) for the centre crack case.

2.7 Normalization

Prior to discretization and numerical solution, equation (2.39) must be normalized, with a natural choice for the stress and length (fig. 1) scales being

$$S_n = \frac{2\mu}{\pi(1+\kappa)} = \frac{E'}{4\pi} \text{ and } l_n = R. \tag{2.44}$$

For edge and centre cracks, $l_n = a$. The following normalized variables are then defined:

$$\begin{array}{lll} S_y{=}\sigma_{yy}^{\infty}/S_n & S_x{=}\sigma_{xx}^{\infty}/S_n & S_{yy}^{\infty\mathrm{h}}(X){=}\sigma_{yy}^{\infty\mathrm{h}}(x)/S_n \\ X{=}x/l_n & B{=}b/l_n & D{=}d/l_n = 1/B. \end{array} \tag{2.45}$$

The stress function is normalized as $F(X,B) = l_n f(x,b;R)$ while the dislocation density is already normalized because, from (2.1), $D(b) = -\frac{\mathrm{d}\delta}{\mathrm{d}b} = -\frac{\mathrm{d}(\delta/l_n)}{\mathrm{d}B}$. The length of the crack relative to the hole is specified by

$$a_n = a/(R+a) \tag{2.46}$$

Table 2: The normalized limits, B_l and B_r for the first integral in equation (2.39) as required by the four crack geometries of fig. 1.

Case	B_l	B_r	l_n
hole (a),(b)	1	$\frac{R+a}{R} = \frac{1}{1-a_n}$	R
edge (c), centre (d)	0	1	a

so that short cracks imply $a_n \to 0$ whilst long cracks have $a_n \to 1$.

The limits on the first integral in (2.39) become B_l and B_r, given in table 2 for the four cases.

After normalization, equation (2.39) becomes

$$\int_{B_l}^{B_r} F(X,B)D(B)\mathrm{d}B - 2\pi k l_n \int_X^{B_r} D(B)\mathrm{d}B = S_{yy}^{\infty\mathrm{h}}(X) \tag{2.47}$$

where, for the hole cases

$$S_{yy}^{\infty\mathrm{h}}(X) = S_y\left(1 + \frac{1}{2X^2} + \frac{3}{2X^4}\right) + S_x\left(\frac{1}{2X^2} - \frac{3}{2X^4}\right). \tag{2.48}$$

For the edge and centre cracks, $S_{yy}^{\infty}(X) = S_y$ only. The main results required from (2.47) are the crack tip stress intensity factor K_{tip} and crack mouth opening $l_n\delta_n(B_l)$. These are

$$\begin{aligned} K_{\mathrm{tip}} &= \frac{E'}{4}\lim_{B\to B_r^-}\left\{\sqrt{2\pi l_n}\sqrt{B_r - B}D(B)\right\} \\ &= \lim_{B\to B_r^+}\left\{\sqrt{2\pi l_n}\sqrt{B - B_r}S_n S_{yy}(B)\right\} \qquad (2.49) \\ \delta_n(B_l) &= \int_{B_l}^{B_r} D(B)\mathrm{d}B. \qquad (2.50) \end{aligned}$$

The first of these demonstrates the $\frac{1}{\sqrt{B_r - B}}$ singularity expected for $D(B)$ for any crack with a non-zero K_{tip}. To overcome this problem, and increase the accuracy of the numerical work by decreasing the discretization intervals as $B \to B_r$ where $D(B)$ changes most rapidly, a variable transformation is made. Following the procedure of Rose, 1987,

$$\begin{aligned} B &= B_r\sin(t) \qquad & \mathrm{d}B &= B_r\cos(t)\mathrm{d}t \\ X &= B_r\sin(u) \qquad & D(B) &= \frac{Q(t)}{B_r\cos(t)} \\ t_l &= \sin^{-1}(B_l/B_r) \qquad & t_r &= \pi/2 \end{aligned} \tag{2.51}$$

and the integral equation becomes

$$\int_{t_l}^{t_r} F\Big(B_r\sin(u), B_r\sin(t)\Big)Q(t)\mathrm{d}t + 2\pi k l_n \int_u^{t_r} Q(t)\mathrm{d}t = S_{yy}^{\infty\mathrm{h}}\Big(B_r\sin(u)\Big). \tag{2.52}$$

The interval $[t_l, t_r]$ is split into N uniform intervals of width δ_t with midpoints $t(j) = t_l + (j - \frac{1}{2})\delta_t$ as in fig. 6. The first integral for $u = t(j)$ can then be split up as $I(j) = \sum_{i=1}^{N}\delta I(j,i)$ where

$$\delta I(j,i) = \int_{t(i-\frac{1}{2})}^{t(i+\frac{1}{2})} Q(t)F\Big(t(j), t\Big)\mathrm{d}t. \tag{2.53}$$

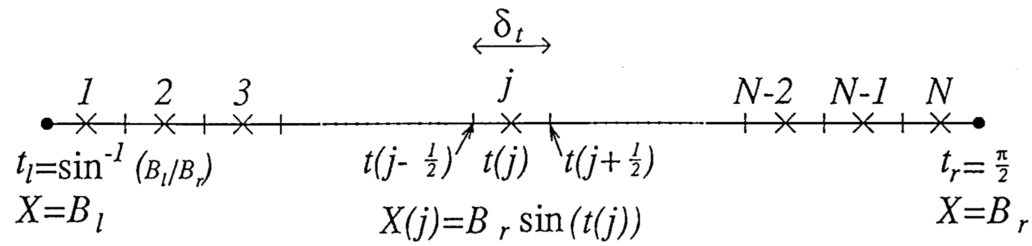

Figure 6: The discretization of the interval $[t_l, t_r]$ showing N intervals, the j^{th} having boundaries $t(j-\frac{1}{2})$ and $t(j+\frac{1}{2})$.

Two approximations are now made: firstly $Q(t)$ is taken as a constant, $Q(i) = Q(t(i))$, over the interval of integration, and secondly the trapezoidal rule is used to evaluate the remaining integral. These give

$$\delta I(j,i) = Q(i)\frac{\delta_t}{2}\Big\{F\Big(t(j), t(i-\frac{1}{2})\Big) + F\Big(t(j), t(i+\frac{1}{2})\Big)\Big\}. \tag{2.54}$$

Particular care is required when $j = i$ because, in this case, the singularity in $F(t(j), t)$ needs to be integrated over. It arises from the term $\frac{1}{X-B}$ in $F(X, B)$. The singular part is thus

$$\delta I^{\text{singular}}(j,j) = Q(j)\int_{t(j)-\frac{\delta_t}{2}}^{t(j)+\frac{\delta_t}{2}} \frac{1}{B_r\Big\{\sin\Big(t(j)\Big) - \sin(t)\Big\}}\mathrm{d}t. \tag{2.55}$$

Changing the variable $t = t(j) + \frac{1}{2}\delta_t v$ and expanding $\sin(t)$ in a Taylor's series about $t(j)$:

$$\begin{aligned}\sin(t) \quad &\approx \quad \sin\Big(t(j)\Big) + \Big(t - t(j)\Big)\cos\Big(t(j)\Big) - \frac{1}{2}\Big(t-t(j)\Big)^2\sin\Big(t(j)\Big) \\ &\qquad -\frac{1}{6}\Big(t-t(j)\Big)^3\cos\Big(t(j)\Big) + \cdots,\end{aligned} \tag{2.56}$$

we obtain

$$\delta I^{\text{singular}}(j,j) = \frac{-Q(j)}{B_r\cos\Big(t(j)\Big)}\int_{-1}^{1}\frac{\mathrm{d}v}{v}\left(1 - \frac{\delta_t}{4}\tan\Big(t(j)\Big)v - \frac{\delta_t^2}{24}v^2 + \cdots\right)^{-1}. \tag{2.57}$$

The integrand may be expanded using the series for $1/(1-\delta)$ and the integral of $\frac{1}{v}$ vanishes by the principal value. The integral of the (third) term proportional to v vanishes too, by symmetry. Just the second term is left, together with terms of order δ_t^3, that is

$$\delta I^{\text{singular}}(j,j) = -\frac{\delta_t}{2}Q(j)\frac{\sin\Big(t(j)\Big)}{\cos\Big(t(j)\Big)} + O(\delta_t^3). \tag{2.58}$$

The same result would have been obtained directly from (2.54), that is the singularity is taken care of by application of that formula for $j = i$.

Turning to the next integral in (2.52), the term due to springs is

$$I^{\text{sp}}(j) = 2\pi k l_n\int_{t(j)}^{t_r} Q(t)\mathrm{d}t = 2\pi k l_n \delta_n(j). \tag{2.59}$$

The trapezoidal rule is again used, but extra care as $t \to t_r$ gives expressions for $Q(t), D(t)$ and $\delta_n(t)$ that extrapolate to $t = t_r$, the one for $Q(t)$ being useful later to calculate K_{tip}.

If, in addition to (2.51) the change $\varepsilon = (\pi/2) - t$ is made, then the $B \to B_r$ expansion of $\delta_n(B)$ becomes

$$\begin{aligned}\delta_n(B \to B_r) &= \Big(\alpha_0 + \alpha_1(B_r - B) + \cdots\Big)\sqrt{B_r - B} \\ &= \sqrt{B_r/2}\,\varepsilon\Big(\alpha_0 + (B_r\alpha_1/2 - \alpha_0/24)\varepsilon^2 + \cdots\Big)\end{aligned} \tag{2.60}$$

and

$$Q(\varepsilon) = \frac{\mathrm{d}\delta_n}{\mathrm{d}\varepsilon} = \sqrt{b_r/2}\Big(\alpha_0(1 - \varepsilon^2/8) + 3\alpha_1 B_r \varepsilon^2/2\Big). \tag{2.61}$$

Substituting in $\varepsilon = \delta_t/2$ and $3\delta_t/2$ gives equations for $Q(N)$ and $Q(N-1)$ respectively, which may be solved for α_0 and α_1:

$$\begin{aligned}\alpha_0 &= \sqrt{\frac{2}{B_r}}\left[\frac{9Q(N) - Q(N-1)}{8}\right] \\ \alpha_1 &= \frac{-1}{3B_r}\sqrt{\frac{2}{B_r}}\left[\frac{Q(N) - Q(N-1)}{\delta_t^2}\right].\end{aligned} \tag{2.62}$$

These may be substituted back into (2.60), leading to

$$\begin{aligned}\delta_n(N) &= \frac{\delta_t}{24}\Big(13Q(N) - Q(N-1)\Big) \\ \delta_n(N-1) &= \frac{\delta_t}{24}\Big(27Q(N) + 9Q(N-1)\Big).\end{aligned} \tag{2.63}$$

The trapezoidal rule, in the form

$$\delta_n(j) = \delta_n(j+1) + \frac{\delta_t}{2}\Big(Q(j) + Q(j+1)\Big) \tag{2.64}$$

is then used in (2.59) to express $I^{\mathrm{sp}}(j)$ as a matrix multiplying the array $Q(i)$:

$$\begin{aligned}I^{\mathrm{sp}}(j) &= 2\pi k l_n \frac{\delta_t}{24}\sum_i M^{\mathrm{sp}}(j,i).Q(i) \\ M^{\mathrm{sp}}(j,i) &= \begin{bmatrix} 12 & 24 & \cdots & 24 & 21 & 27 \\ 0 & 12 & \cdots & 24 & 21 & 27 \\ \cdots & \cdots & \cdots & \cdots & \cdots & \cdots \\ 0 & 0 & \cdots & 12 & 21 & 27 \\ 0 & 0 & \cdots & 0 & 9 & 27 \\ 0 & 0 & \cdots & 0 & -1 & 13 \end{bmatrix}.\end{aligned} \tag{2.65}$$

Setting

$$\begin{aligned}M^0(j,i) &= \frac{\delta_t}{2}\left\{F\Big(t(j), t(i - \frac{1}{2})\Big) + F\Big(t(j), t(i + \frac{1}{2})\Big)\right\} \\ C(j) &= S_{yy}^{\infty\mathrm{h}}\Big(X(j)\Big),\end{aligned} \tag{2.66}$$

a matrix equation is obtained for $Q(i)$:

$$\begin{aligned}\sum_i M(j,i).Q(i) &= C(j) \\ M(j,i) &= M^0(j,i) - 2\pi k l_n \frac{\delta_t}{24} M^{\mathrm{sp}}(j,i).\end{aligned} \tag{2.67}$$

2.8 Normalized K_{tip} and Crack Mouth Opening

Returning to (2.49) and substituting in the derivative of (2.60) for $D(B)$, the crack tip stress intensity factor K_{tip} may be given in a similar normalized form to that of Rose, 1987, that is

$$\begin{aligned} K_{\text{tip}} &= \sigma_{yy}^{\infty}\sqrt{\pi a}F_n(ka; a_n; \lambda) \\ F_n(ka; a_n; \lambda) &= \sqrt{\frac{l_n}{2a}}\left(\frac{\pi}{S_y}\right)\alpha_0 = \sqrt{\frac{1-a_n}{a_n}}\left(\frac{\pi}{S_y}\right)\alpha_0 \end{aligned} \tag{2.68}$$

with the last equality for the hole cases only. For edge and centre cracks, the $\sqrt{\frac{1-a_n}{a_n}}$ factor is replaced by $1/\sqrt{2}$. Equation (2.62) provided an expression for α_0.

Both the normalization for K_{tip} and the dimensionless spring constant ka, could have been selected differently, for example the a in $\sigma_{yy}^{\infty}\sqrt{\pi a}$ could justifiably be replaced by $2R + a$ for the single crack from a hole, and $R + a$ for the symmetric double crack. The spring constant could have been kR but the chosen normalizations lead most readily to the asymptotic limits of small hole, large hole, weak springs and stiff springs.

The crack mouth opening $\delta(b_l)$ may also be normalized as

$$\begin{aligned} \delta(b_l) &= l_n\delta_n(B_l) = \left(\frac{4\sigma_{yy}^{\infty}a}{E'}\right)V_n(ka; a_n; \lambda) \\ V_n(ka; a_n; \lambda) &= \frac{l_n}{a}\left(\frac{\pi}{S_y}\right)\delta_n(B_l) = \frac{1-a_n}{a_n}\left(\frac{\pi}{S_y}\right)\delta_n(B_l). \end{aligned} \tag{2.69}$$

The numerical integration, (2.64), does not give $\delta_n(B_l)$ because $\delta_n(j = 1)$ corresponds to $\delta_n(t_l + \delta_t/2)$ from fig. (6). We choose, in preference to the trapezoidal rule,

$$\delta_n(t_l) = \delta_n(1) + \frac{\delta_t}{2}Q(1) \tag{2.70}$$

to be substituted into the previous equation. Again, edge and centre cracks do not have the $\frac{1-a_n}{a_n}$ factor, and the dependence on λ is trivial for it has no effect in these cases.

3 ASYMPTOTIC LIMITS: K_{tip}

As indicated previously, there are several asymptotic limiting cases for the cracks emanating from a hole, both in terms of the geometry, R relative to a, specified by a_n, and the spring stiffness indicated by ka. In the following sections, stiff springs will be treated first, large holes or short cracks next, small holes or long cracks, and finally weak springs.

3.1 Stiff Springs

Here, the springs are so stiff that k^{-1} is small relative to both a and R, so that from Rose, 1987, $K_{\text{tip}} \to \sigma_{yy}^{\text{tip}}/\sqrt{k}$. From equations (2.27) (and 2.45),

$$\sigma_{yy}^{\text{tip}} = \sigma_{yy}^{\infty}\left\{1 + \frac{1}{2}(1+\lambda)\left(\frac{R}{R+a}\right)^2 + \frac{3}{2}(1-\lambda)\left(\frac{R}{R+a}\right)^4\right\} \tag{3.1}$$

so that

$$F_n(ka \to \infty; a_n; \lambda) \to \frac{1}{\sqrt{\pi ka}}\left(1 + \frac{1}{2}(1+\lambda)(1-a_n)^2 + \frac{3}{2}(1-\lambda)(1-a_n)^4\right). \tag{3.2}$$

3.2 Large R or Small a

The simplest limit is $R \to \infty$ relative to a, or $a_n \to 0$. In this case, both hole configurations approximate to an edge crack of length a, loaded by a stress given by the $R/x \to 1$ limit of (2.27):

$$\sigma_{yy}(x) \to 3\sigma_{yy}^{\infty} - \sigma_{xx}^{\infty} = (3-\lambda)S_n S_y. \tag{3.3}$$

In this case,

$$F_n(ka; a_n \to 0; \lambda) \to (3-\lambda)F_n^{\text{edge}}(ka). \tag{3.4}$$

For stiff springs, from (3.2), the limit is

$$F_n(ka \to \infty; a_n \to 0; \lambda) \to \frac{1}{\sqrt{\pi ka}}\big(3 - \lambda - (7-5\lambda)a_n\big). \tag{3.5}$$

3.3 Small R or large a

As the crack becomes much longer than the hole radius, $a_n \to 1$, both hole cases approach (different) centre crack geometries, but the asymptotes may be taken in different ways for each case. Although they limit to the same in each case, they produce different forms for (2.68) and (2.69).

One procedure is to take the correspondences shown in fig. 7 (a) and (b) for the single and double cracks respectively, simple in terms of variable substitutions, but not as accurate as cases (c) and (d), which should hold further from the $a_n \to 1$ limit.

Taking fig. 7 (c), the limit for K_{tip} becomes the fully reinforced ($c/a \to 0$) treatment of Rose, 1987, where effects due to the hole at the other end of the crack, including

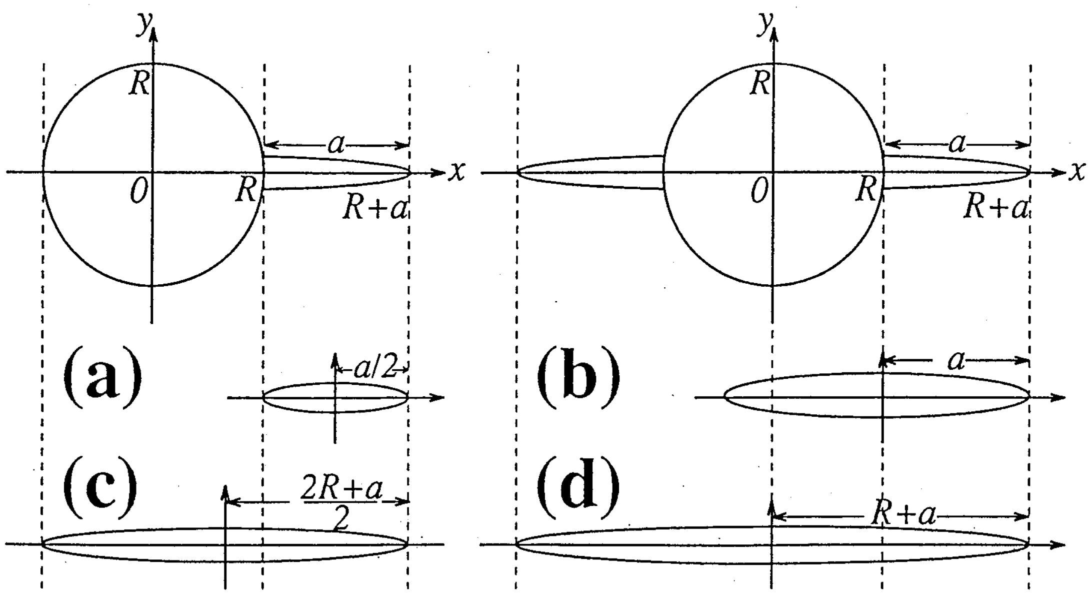

Figure 7: Possible correspondences between the hole configurations and $a_n \to 1$ long crack limits. In cases (**a**) and (**b**), a in the centre crack case becomes $a/2$ and a for the single and double crack cases respectively. In (**c**), a is replaced by $(2R+a)/2$, and for (**d**), a becomes $R+a$.

the stress concentration of (2.27) and the lack of springs across the hole, become negligible.

For no springs and correspondence (c), $K_{\text{tip}} = \sigma_{yy}^{\infty}\sqrt{\pi(2R+a)/2}$ whereupon

$$F_n(0; a_n \to 1; \lambda) \to \frac{1}{\sqrt{2}}\sqrt{\frac{2}{a_n} - 1} \approx \frac{1}{\sqrt{2}}\Big(1 + (1 - a_n)\Big). \tag{3.6}$$

As the springs become stiff, we take $a_n \to 1$ in (3.2):

$$F_n(ka \to \infty; a_n \to 1; \lambda) \to \frac{1}{\sqrt{\pi k a}}\Big(1 + \frac{1}{2}(1+\lambda)(1-a_n)^2\Big) \tag{3.7}$$

which is the same as Rose, 1987 for $\lambda = 0$.

The last equation would still hold for the double crack, case (d) in fig. 7, but equation (3.6) wouldn't because K_{tip} is now given by $\sigma_{yy}^{\infty}\sqrt{\pi(R+a)}$. Instead,

$$F_n(0; a_n \to 1; \lambda) \to \frac{1}{\sqrt{a_n}} \approx 1 + \frac{1}{2}(1 - a_n). \tag{3.8}$$

3.4 Weak Springs, $ka \to 0$ Limit

Single and double crack hole cases are presented by Tada *et al.*, 1985 for no springs, $ka = 0$, where s is here represented by a_n, and σ by σ_{yy}^{∞}. The other variables, R, a and λ are the same.

The single crack case, from page 19.2 in Tada *et al.*, 1985, is presented as

$$F_n(0; a_n; \lambda) \quad = \quad (1-\lambda)F_0(a_n) + \lambda F_1(a_n)$$

$$F_0(a_n) = \left(1 + 0.2(1-a_n) + 0.3(1-a_n)^6\right)F_1(a_n) \tag{3.9}$$
$$F_1(a_n) = 2.243 - 2.640a_n + 1.352a_n^2 - 0.248a_n^3.$$

In particular, as $a_n \to 1$, these have the limits

$$F_0(a_n \to 1) \to 0.707 + 0.680(1-a_n) \tag{3.10}$$
$$F_1(a_n \to 1) \to 0.707 + 0.821(1-a_n)$$

which are close to (3.6). The other limit for a_n produces

$$F_n(0; a_n \to 0; \lambda) \to 1.1215(3-\lambda) - (8.446 - 5.806\lambda)a_n. \tag{3.11}$$

For the symmetric double crack case, Tada *et al.*, 1985, page 19.1 presents $F_n(0; a_n; \lambda)$ as before but with

$$F_0(a_n) = 0.5(3-a_n)\left(1 + 1.243(1-a_n)^3\right) \tag{3.12}$$
$$F_1(a_n) = 1 + 0.5(1-a_n) + 0.743(1-a_n)^3.$$

In this case, as $a_n \to 1$, both F_0 and F_1 approach the same limit as (3.8). The $a_n \to 0$ limit is

$$F_n(0; a_n \to 0; \lambda) \to 1.1215(3-\lambda) - (6.715 - 3.986\lambda)a_n. \tag{3.13}$$

The F_0 and F_1 functions in both cases are accurate to within 1 % according to Tada *et al.*, 1985.

Tada *et al.*, 1985, page 8.1 also presents the edge crack, essentially the limit of the above two cases as $a_n \to 0$, without the stress concentration factor of $(3-\lambda)$. For the edge crack, λ has no effect, and

$$F_n^{\text{edge}}(ka = 0) = 1.1215. \tag{3.14}$$

Later arguments for small ka indicate that, for all geometries, F_n may be expanded in the series

$$F_n(ka \to 0; a_n; \lambda) \to a_F(a_n; \lambda) - b_F(a_n; \lambda)ka + c_F(a_n; \lambda)(ka)^2, \tag{3.15}$$

where a_F gives $F_n(0; a_n; \lambda)$ as reproduced from Tada *et al.*, 1985 above. A value may be calculated for b_F in the edge and centre crack cases following the self-consistent perturbation approach of the next section. For the hole cases it is calculated numerically by fitting (3.15) to F_n calculated for small ka. Rose, 1987 gives the numerical value $c_F = 2.110$ for the centre crack case.

3.5 Self-Consistent Perturbation Theory for Small ka

There are three ideas underpinning this approach, the first being that K_{tip} may be calculated as a superposition of the K_{tip} values produced by the contributing stresses: those due to the applied load and the springs. The second is that those stresses acting closest to the crack tip contribute most to K_{tip}, hence the crack opening profile needs to be known most accurately there to produce an accurate value for $K_{\text{tip}}^{\text{sp}}$, the contribution of the springs. Thirdly, we take the crack profile to be the same as the unsprung crack with the same loading geometry, but scaled (self-consistently) to give the correct K_{tip} according to equation (2.49). These ideas will be illustrated for the centre crack case which can be treated analytically.

If $g(x;a)$ is K_{tip} for a crack of length specified by a (length is $2a$ for the centre crack) for a unit applied point force at x on the crack face, then the total stress intensity factor is

$$K_{\text{tip}} = \int_{\text{crack}} \sigma(x) g(x;a) \mathrm{d}x. \tag{3.16}$$

Here, $\sigma(x)$ is the net stress on the crack face due to the applied load and the springs. Using the first idea above, it may be split as

$$\sigma(x) = \sigma_{yy}^{\infty}(x) - \frac{1}{2} E' k \delta(x) \tag{3.17}$$

where equations (2.3) and (2.27) have been used. This leads to

$$\begin{aligned} K_{\text{tip}} &= K_0 - \frac{1}{2} E' k \int_{\text{crack}} \delta(x) g(x;a) \mathrm{d}x \\ K_0 &= \int_{\text{crack}} \sigma_{yy}^{\infty}(x) g(x;a) \mathrm{d}x. \end{aligned} \tag{3.18}$$

For the centre crack, $\sigma_{yy}^{\infty}(x)$ is a constant, σ_{yy}^{∞}.

If ka is small, then to lowest order $\delta(x)$ will be the same as if there were no springs. This would be sufficient for it enters into the K_{tip} correction term only. Ideas two and three above suggest that we can do better than this, for this $\delta(x)$ is known to produce K_0 by equation (2.49). For the centre crack and uniaxial remote tension, Tada *et al.*, 1985, page 5.1a gives

$$\begin{aligned} \delta_0(x) &= \frac{4\sigma_{yy}^{\infty} a}{E'} \sqrt{1-(x/a)^2} = \frac{4\sigma_{yy}^{\infty}}{E'} \delta'(x) \\ K_0 &= \sigma_{yy}^{\infty} \sqrt{\pi a}. \end{aligned} \tag{3.19}$$

We replace K_0 in the second equation by K_{tip}, and substitute for σ_{yy}^{∞} in the first, thereby accomplishing the third idea above. The result is

$$K_{\text{tip}} = K_0 - \frac{2K_{\text{tip}} ka}{\sqrt{\pi a}} \int_{\text{crack}} \delta'(x) g(x;a) \mathrm{d}(x/a). \tag{3.20}$$

Substituting in $\delta'(x)$ from above, and

$$g(x;a) = \frac{2}{\sqrt{\pi a}} \frac{1}{\sqrt{1-(x/a)^2}} \tag{3.21}$$

from Tada *et al.*, 1985, pages 5.11 and 5.11a for point forces applied at x and $-x$ in the centre crack, the equation for K_{tip} reduces to

$$\begin{aligned} K_{\text{tip}} &= K_0 - \frac{4ka}{\pi} K_{\text{tip}} \int_{x/a=0}^{1} \mathrm{d}(x/a) \\ &\approx K_0 \Big(1 - (4/\pi) ka + (16/\pi^2)(ka)^2 + \cdots \Big). \end{aligned} \tag{3.22}$$

This compares to the Rose, 1987 form

$$K_{\text{tip}}/K_0 = 1 - \frac{4}{\pi} ka + 2.110 (ka)^2 + \cdots. \tag{3.23}$$

The first order term would have been the same even if the self-consistent replacement of K_0 by K_{tip} had not been done, but that would not have given a second order term.

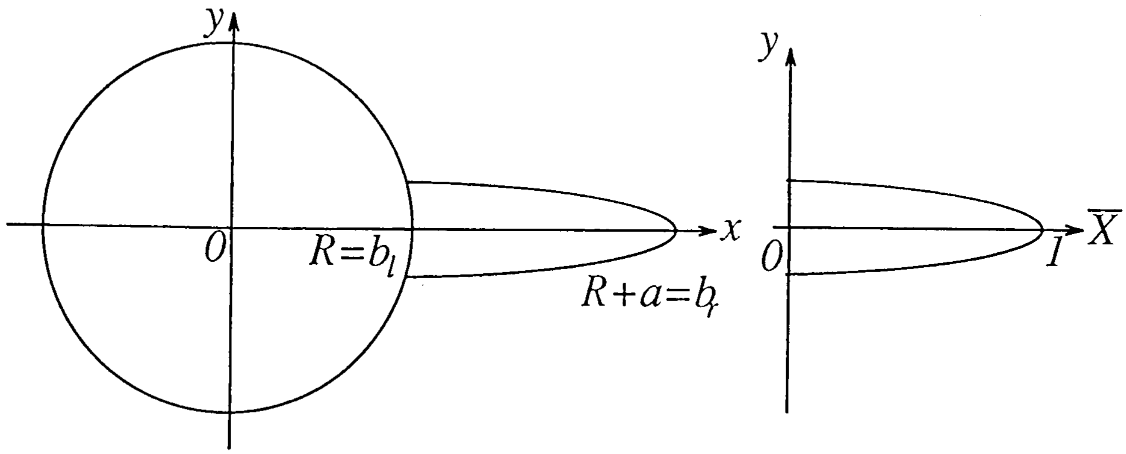

Figure 8: Hole co-ordinates related to those for the edge, corresponding to $a_n \to 0$. The crack, extending from $R = b_l$ to $R + a = b_r$ is treated like an edge crack from $\overline{X} = 0$ to 1. Note that the normalization is different to equation (2.45) but that it is also applied to the double crack case.

The edge crack may be treated similarly as the $\delta(x)$ and $g(x;a)$ functions are given (approximately) by Tada *et al.*, 1985, pages 8.1a, 8.3. Just presenting the equations,

$$\begin{aligned}
\delta'(x) &= a\sqrt{1-(x/a)^2}D(x/a) \\
D(X) &= 1.454 - 0.727X + 0.618X^2 - 0.224X^3 \\
g(x;a) &= \frac{2}{\sqrt{\pi a}}\frac{1}{\sqrt{1-(x/a)^2}}G(x/a) \\
G(X) &= 1.3 - 0.3X^{5/4} \\
K_{\text{tip}} &= K_0 - \frac{4ka}{1.1215\pi}K_{\text{tip}}\int_0^1 D(X)G(X)\mathrm{d}X.
\end{aligned} \tag{3.24}$$

The integral equals 1.4551 making the final result

$$K_{\text{tip}} = \sigma_{yy}^{\infty}\sqrt{\pi a}\Big(1.1215 - 1.8516ka + 3.0587(ka)^2 + \cdots\Big). \tag{3.25}$$

The other cases examined here, single crack from a hole and symmetric double crack from a hole, can not be treated so simply because the functions $\delta(x)$ and $g(x;a;R)$ are not known. The best that can be done is to fit appropriate functions to numerically calculated profiles for $\delta(x)$, and to seek an approximation for $g(x;a;R)$. Both cracked hole cases will be related to the edge crack treatment as illustrated in fig. 8. This is the $a_n \to 0$ correspondence, to be compared to fig. 7 which was for $a_n \to 1$. In the case of uniaxial tension, $\lambda = 0$, the correspondence may be summed up as

$$\begin{aligned}
\delta(x) &= \frac{4\sigma_{yy}^{\infty}a}{E'}\sqrt{1-\overline{X}^2}D(\overline{X}) \\
a &= b_r - b_l = (R+a) - R \\
\overline{X} &= (x-b_l)/(b_r-b_l) = (x-R)/a.
\end{aligned} \tag{3.26}$$

Noting the original normalizations (2.45), the function $D(\overline{X})$ is obtained using

$$\overline{X} = \frac{X - B_l}{B_r - B_l} = \left(\frac{1-a_n}{a_n}\right)(X-1), \text{ where } B_l = 1 \tag{3.27}$$

Table 3: The cubic function $D(\overline{X})$ fitted using least squares to the numerical crack profiles for various a_n. The normalizations for $\overline{X}$ and $D(\overline{X})$ are given by equations (3.27).

a_n	$D(\overline{X})$ for an edge crack
edge	$1.454 - 0.727\overline{X} + 0.618\overline{X}^2 - 0.224\overline{X}^3$
$3\times$ edge	$4.362 - 2.181\overline{X} + 1.854\overline{X}^2 - 0.672\overline{X}^3$
a_n	$D(\overline{X})$ for a single crack from a hole
0.1	$3.605 - 1.787\overline{X} + 1.399\overline{X}^2 - 0.499\overline{X}^3$
0.5	$1.720 - 0.871\overline{X} + 0.701\overline{X}^2 - 0.245\overline{X}^3$
0.9	$0.523 + 0.493\overline{X} - 0.313\overline{X}^2 + 0.083\overline{X}^3$
a_n	$D(\overline{X})$ for a double crack from a hole
0.1	$3.626 - 1.798\overline{X} + 1.408\overline{X}^2 - 0.502\overline{X}^3$
0.5	$1.983 - 1.017\overline{X} + 0.767\overline{X}^2 - 0.262\overline{X}^3$
0.9	$1.139 - 0.262\overline{X} + 0.330\overline{X}^2 - 0.153\overline{X}^3$
0.9*	$1.137 - 0.257\overline{X} + 0.322\overline{X}^2 - 0.149\overline{X}^3$

* Values calculated using $n = 100$ points indicate degree of convergence, and accuracy obtained by $n = 200$.

$$D(\overline{X}) = \frac{E'}{4\sigma_{yy}^{\infty}}\frac{R\delta_n(X)}{b_r - b_l}\frac{1}{\sqrt{1-\overline{X}^2}} = \frac{\pi}{S_y}\frac{1-a_n}{a_n}\frac{\delta_n(\overline{X})}{\sqrt{1-\overline{X}^2}}.$$

Cubic polynomials were then fitted to $D(\overline{X})$ using least squares as listed in table 3. These functions, for both hole cases, are plotted in fig. 9. The edge, 3 times edge, and centre crack functions are plotted for comparison. The functions are particularly smooth, and the interpolations should be comparable in accuracy to the edge case. Both hole cases approach 3 times the edge case as $a_n \to 0$, but only the double crack case approaches the centre crack at the other limit. This is because the single crack case approaches a centre crack of full length a rather than $2a$ in the $a_n \to 1$ limit. $\overline{X} = 0$ is a closed end of the crack in this case whereas it is the middle of the crack in the double crack case. For the single crack and $a_n \to 0$, $D(\overline{X} = 0) \to 0$ and $D(\overline{X} = 1) \to 1/\sqrt{2}$.

The crack profile may also be expressed using the correspondences of fig. 7 (c) and (d). For the single crack, this gives a function $D_2(\overline{X_2})$ which is almost constant over most of the $\overline{X_2}$ range, whilst correspondence 7 (a) diverged for $\overline{X_2} \to 0$. Still on correspondence 7 (c), equations 3.27 are replaced by

$$\begin{aligned}
\overline{X_2} &= \frac{2x-a}{2R+a} = \frac{2(1-a_n)}{2-a_n}(X+1) - 1 = \frac{2a_n}{2-a_n}(\overline{X}-1)+1 \\
D_2(\overline{X_2}) &= \frac{E'}{4\sigma_{yy}^{\infty}}\frac{2R\delta_n(x)}{2R+a}\frac{1}{\sqrt{1-\overline{X_2}^2}} \qquad (3.28)\\
&= \frac{\pi}{S_y}\frac{2(1-a_n)}{2-a_n}\frac{\delta_n(\overline{X})}{\sqrt{1-\overline{X_2}^2}} = \sqrt{(1+\overline{X})\Big/\Big(\overline{X}-2+2/a_n\Big)}\,D(\overline{X}).
\end{aligned}$$

These functions are shown in fig. 10. They are more nearly constant than $D(\overline{X})$

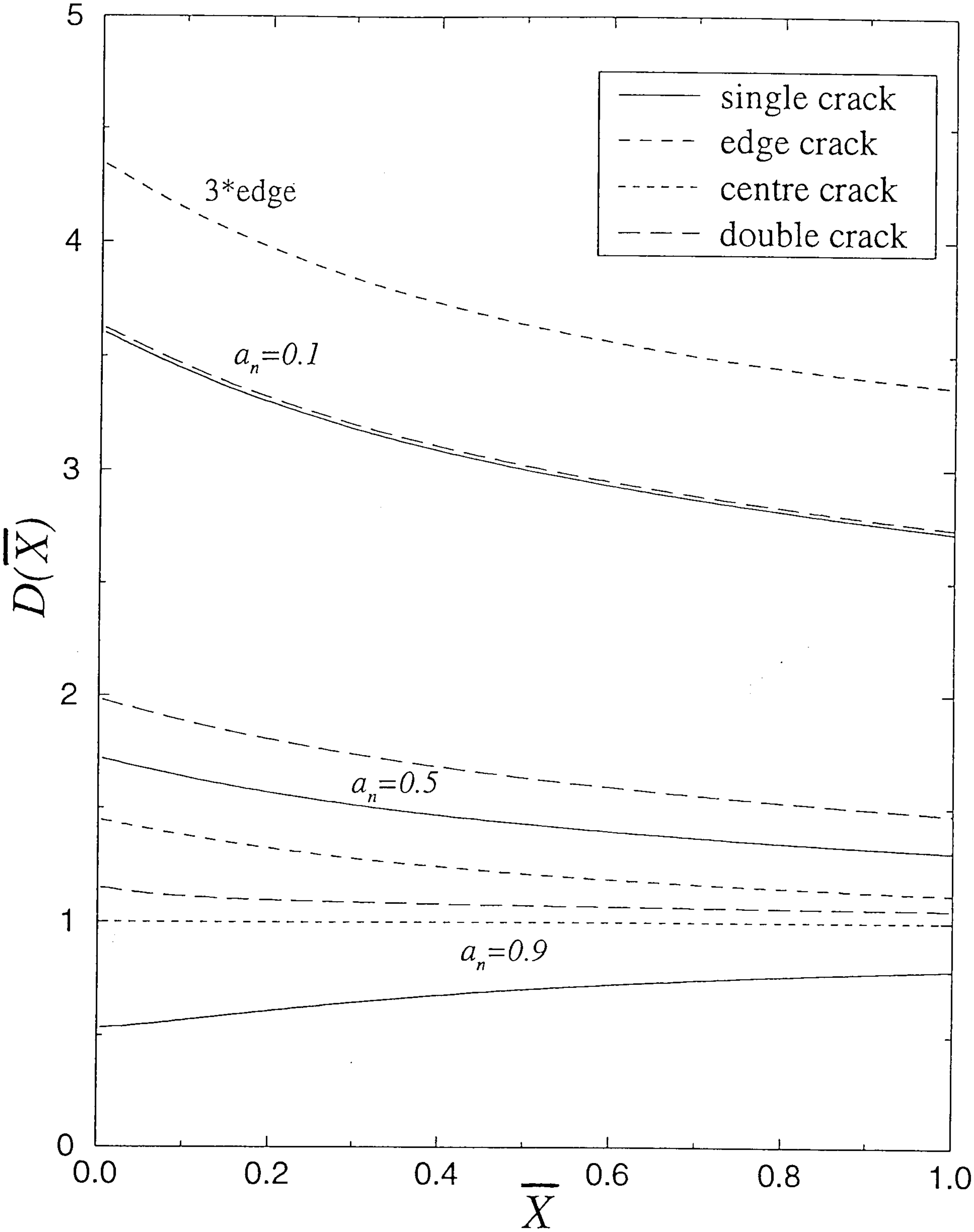

Figure 9: The function $D(\overline{X})$ from equation (3.27) for $a_n = 0.1, 0.5$, and 0.9 compared with the centre and edge crack functions. Here $\lambda = 0$ for both hole cases.

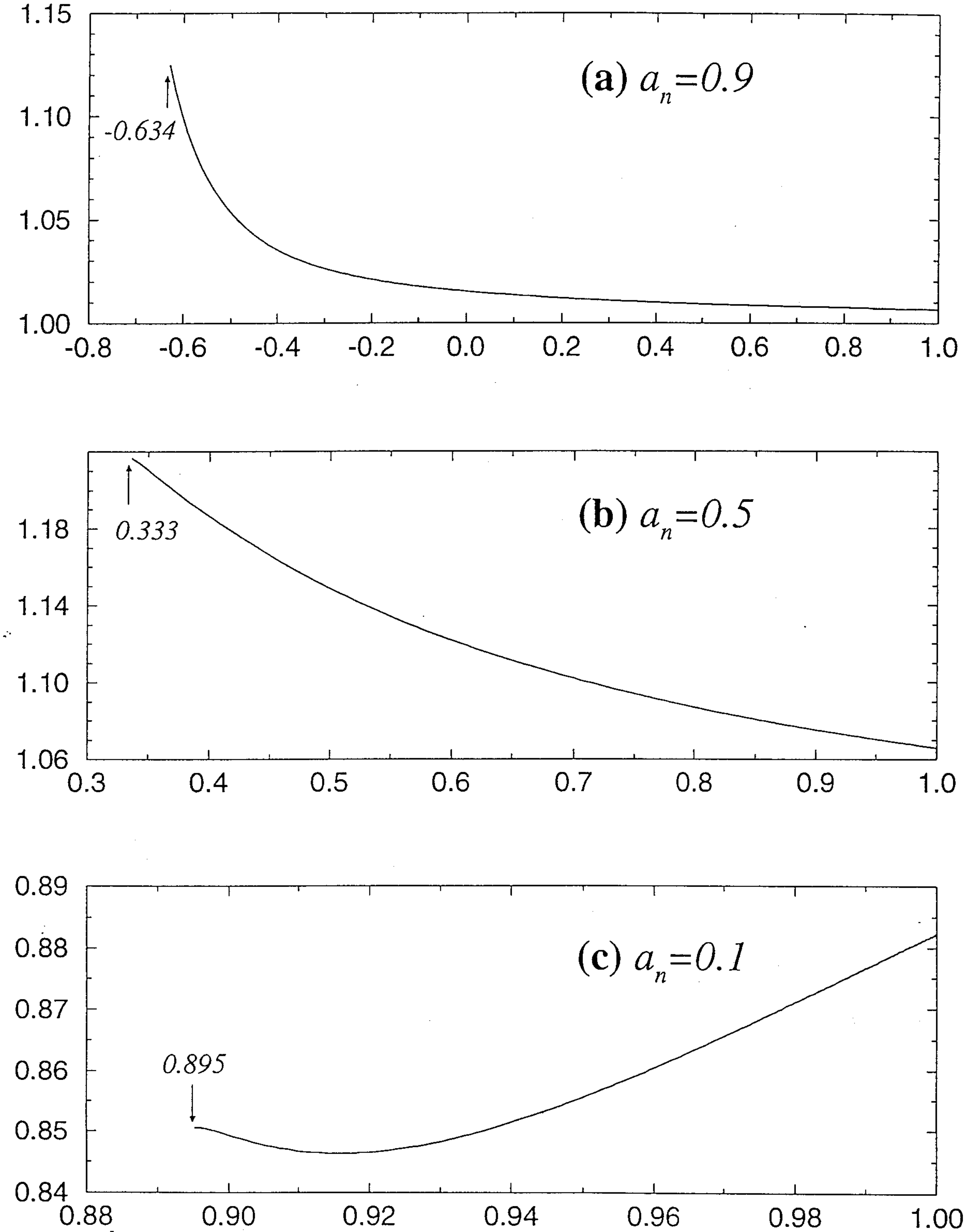

Figure 10: The functions $D_2(\overline{X_2})$, equations (3.28), for $a_n = 0.1, 0.5$, and 0.9 for a single crack from a hole. Note the expanded D_2 (vertical) axis in each case. The arrows indicate $\overline{X_2}$ values corresponding to $\overline{X} = 0$.

(note the expanded scale on fig. 10), but the rapid change as $\overline{X}_2 \to 0$ for $a_n = 0.9$ may cause fitting problems. As mentioned earlier though, the profile has to be most accurate near the crack tip. In this case, and checks would have to be made to verify it, the benefit of near-constancy over most of the $\overline{X}_2$ range may override the problems at $\overline{X} = 0$.

Turning to the double crack case, the preferred correspondence is given in fig. 7 (d). In this case, the normalizations are

$$\begin{aligned} \overline{X_3} &= \frac{x}{R+a} = (1-a_n)X = a_n(\overline{X}-1)+1 \\ D_3(\overline{X_3}) &= \frac{E'}{4\sigma_{yy}^{\infty}} \frac{R\delta_n(x)}{R+a} \frac{1}{\sqrt{1-\overline{X_3}^2}} \\ &= \frac{\pi}{S_y}(1-a_n)\frac{\delta_n(\overline{X_3})}{\sqrt{1-\overline{X_3}^2}} = \sqrt{(1+\overline{X})/\big(\overline{X}-1+2/a_n\big)}D(\overline{X}). \end{aligned} \tag{3.29}$$

These $D_3(\overline{X_3})$ functions are plotted in fig. 11 for the same a_n as before. They have no advantages over the functions $D(\overline{X})$ which are thus preferred because they are well behaved as $a_n \to 0$ and 1.

We thus have $D(\overline{X})$ functions for both hole cases that are as reliable as $D(X)$ for the edge case, but we still need functions analogous to $G(X)$ for the edge crack. These are not so easily obtained, as K_{tip} for a unit point force applied to the crack faces is required here, whereas for $D(X)$, the information was already available through the crack profile. A separate calculation would be required, beyond the scope of this piece of work. We may expect that $g(x;a;R)$ for the single crack from a hole, lies between the limiting edge and centre crack cases of fig. 12. These correspondences have been presented in equations (3.27) and (3.28), so only the normalizations for the $g(x;a;R)$ functions need be given. The edge case was presented in equations (3.24). The function $G(X)$ given there should be an upper limit for the hole cases because it gives K_{tip} assuming the crack is from an edge. With either hole case, the material on the opposite side of the hole to K_{tip} will act to reduce K_{tip} to less than this estimate.

For both hole cases, a lower bound for $g(x;a;R)$ is found by assuming the hole is part of a centre crack as in fig. 7 (c) and (d). This is because removal of material to form the hole would allow some relaxation at the point of application of the point force, and increase K_{tip}.

Looking at the single crack case first, the approximation requires $g(x;a;R)$ for a point force acting on a centre crack, and not the symmetric pair that were used for the centre crack case (equation 3.21). Tada *et al.*, 1985, page 5.10 gives, for a centre crack of length $2a$ and point force at x,

$$g^c(x;a) = \frac{2}{\sqrt{\pi a}} \frac{1}{\sqrt{1-(x/a)^2}} \frac{1}{2}\big(1+x/a\big). \tag{3.30}$$

Here, the first two factors are the function from (3.21), separated out to facilitate later work. We use the same substitutions as (3.28), where x/a above becomes $\overline{X_2}$

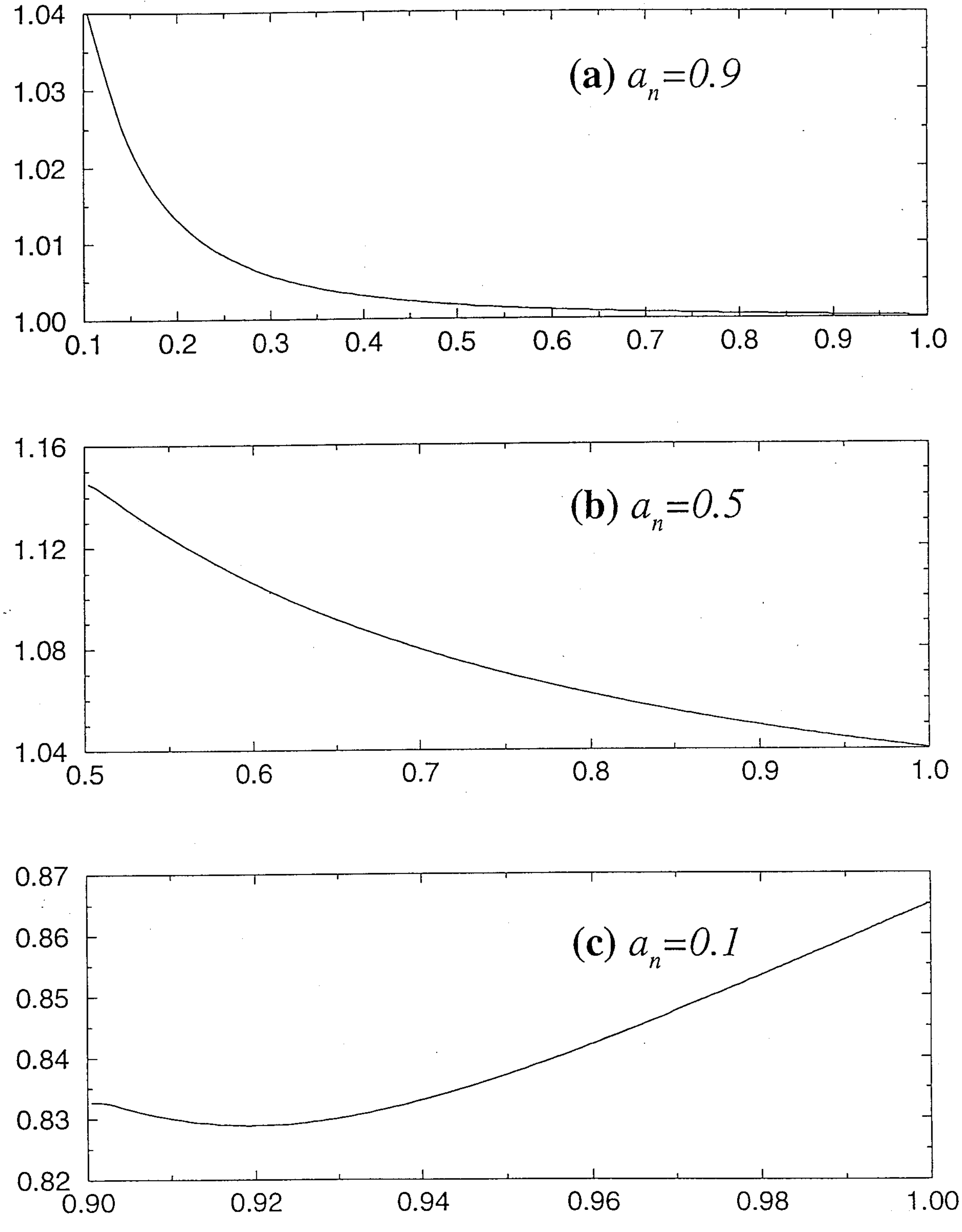

Figure 11: The functions $D_3(\overline{X_3})$ for the symmetric double crack from a hole case. The functions are shown for $a_n = 0.1, 0.5$ and 0.9. These are not really any more useful than the $D(\overline{X})$ functions of fig. 9.

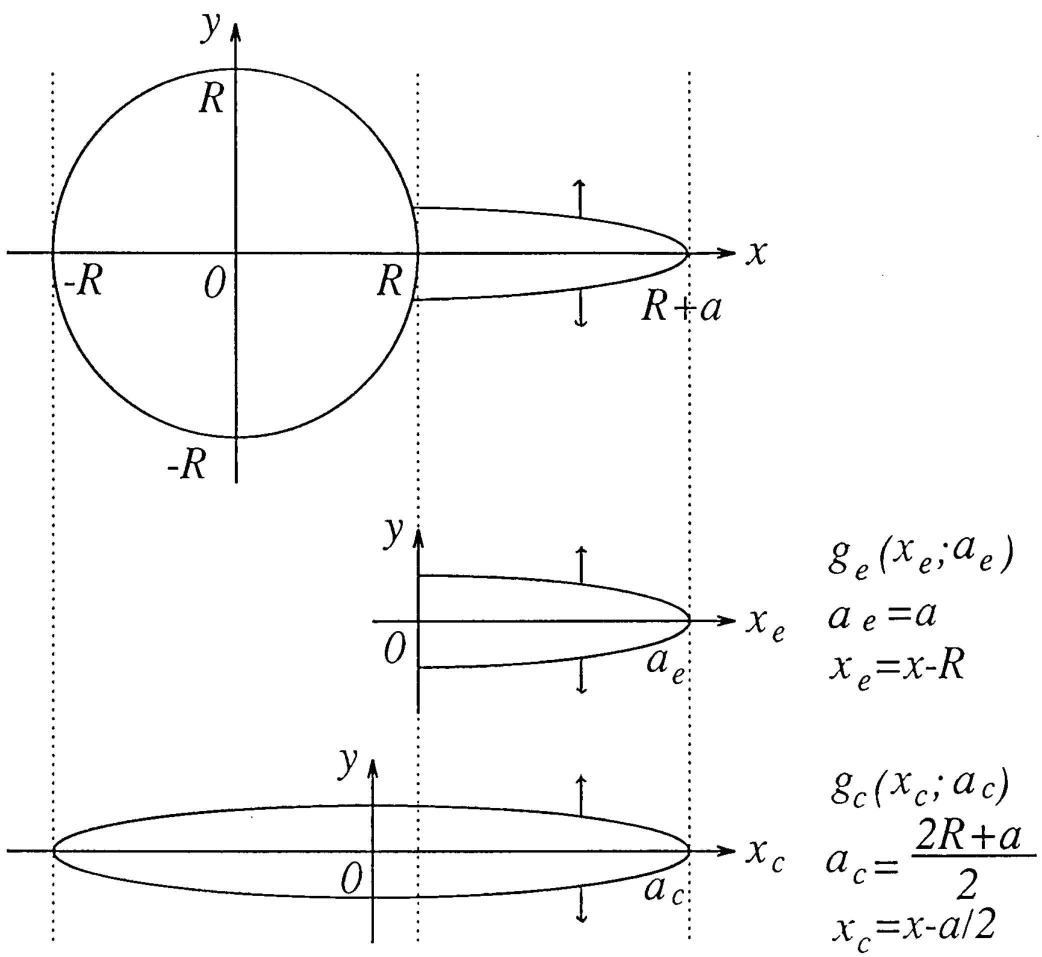

Figure 12: The function $g(x;a;R)$ for the single crack hole case would be expected to lie between the edge and centre crack limits, $g^e(x_e;a_e)$ and $g^c(x_c;a_c)$ respectively, as shown.

and a is replaced by $(2R+a)/2$. The result is

$$g(\overline{X_2}) = \frac{2}{\sqrt{\pi\left(\frac{2R+a}{2}\right)}} \frac{1}{\sqrt{1-\overline{X_2}^2}} \frac{1}{2}\left(1+\overline{X_2}\right). \tag{3.31}$$

To enable comparison with the edge crack (maximum bound), the edge-crack normalization is introduced. From equation 3.24,

$$\begin{aligned} g(\overline{X_2}) &= \frac{2}{\sqrt{\pi a\left(1-\overline{X}^2\right)}} G_2(\overline{X_2}) \qquad (3.32) \\ G_2(\overline{X_2}) &= \sqrt{\frac{a}{2(2R+a)}}\sqrt{\frac{1-\overline{X}}{1-\overline{X_2}}}\sqrt{(1+\overline{X})(1+\overline{X_2})}. \end{aligned}$$

The relationship between $\overline{X}$ and $\overline{X_2}$ was given in equations (3.28). Using this, $G_2(\overline{X_2})$ can be expressed as a function of $\overline{X}$,

$$G_2(\overline{X}) = \sqrt{\frac{a_n/2}{2-a_n}}\sqrt{(\overline{X}+1)(\overline{X}-2+2/a_n)}, \tag{3.33}$$

which is a hyperbola. It is plotted for several a_n along with $G(\overline{X})$ in fig. 13.

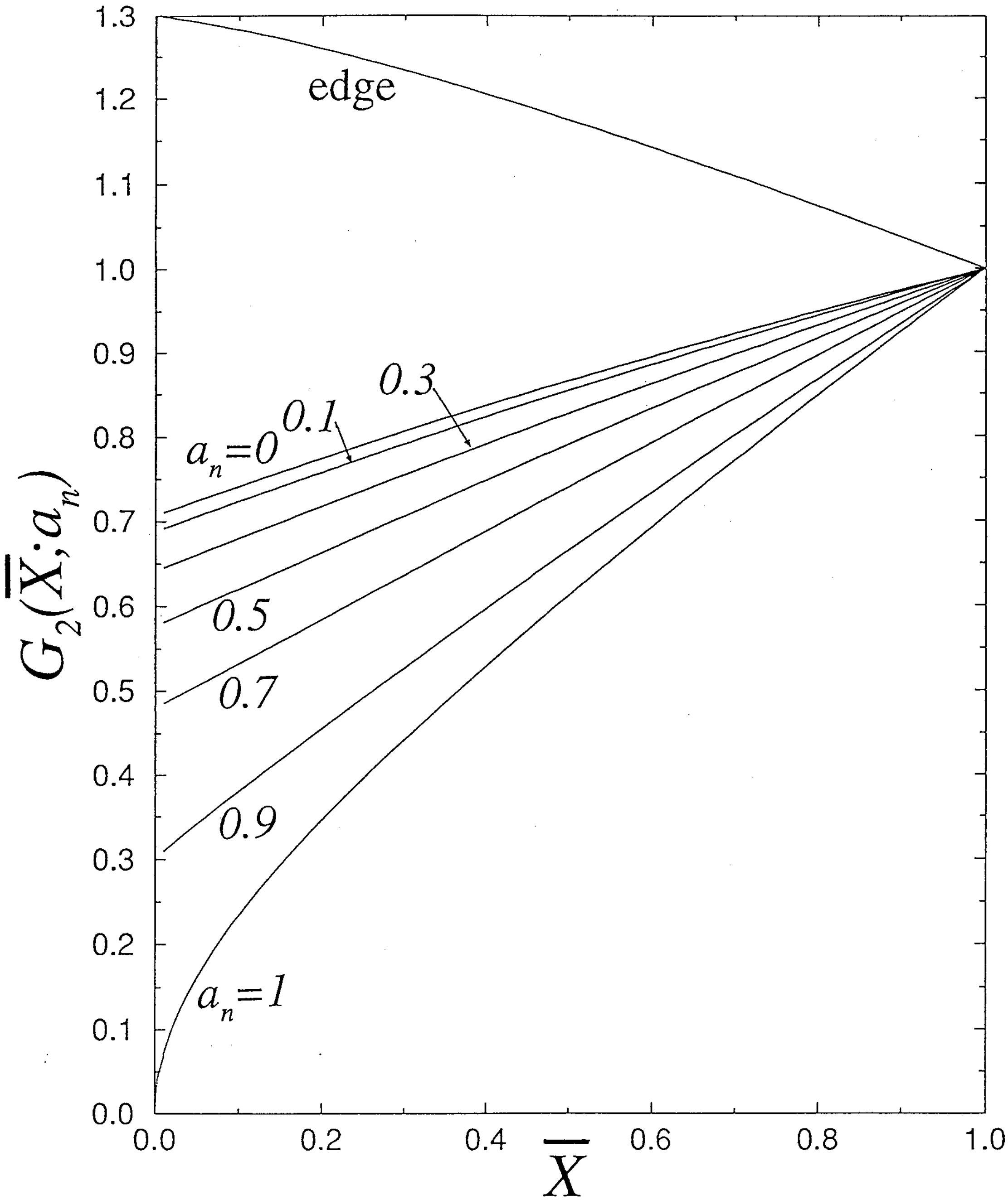

Figure 13: The functions $G(\overline{X})$ (edge approximation) and $G_2(\overline{X})$ (approximating to a centre crack) for the single crack from a hole. The latter function is shown for several a_n, and is part of a hyperbola in each case. The true function would lie between $G(\overline{X})$ and $G_2(\overline{X})$ for each value of a_n.

It is clear from that figure that these bounds are too wide to be useful: the range of possible G functions is so great that first order coefficients in the small ka expansion would be poorly specified here. We may as well take $G(\overline{X}) \equiv 1$ in the integral replacing (3.24) for the single crack from a hole, for it is certainly within the bounds. Given this uncertainty, this part of the investigation was not carried any further, and $G_3(\overline{X_3})$ functions (see equation 3.29) for the double crack case were not examined.

4 NUMERICAL RESULTS AND INTERPOLATION FORMULAE FOR K_{tip}

In this section, the numerical results for $F_n(ka; a_n; \lambda)$ will be presented. They have been calculated for a_n in steps of 0.1, for $\lambda = 0$ and 1, and for both hole cases, (fully bridged) centre and edge cracks. These are shown in fig 14, and tabulated in appendix A.1. In many cases, it may be sufficient to interpolate in this table.

A simpler method of presenting and using this data is to construct interpolation formulae against ka, given a_n and λ, and to tabulate only the parameters of these formulae. Before proceeding to these, it is useful to consider a "map" of the availability of asymptotic limits against which the numerical results may be verified. These are presented in fig 15. They also serve to indicate suitable forms for the interpolation formulae, which have been fitted following the method of Rose, 1987. The parameters are presented in fig 16 and tabulated in appendix A.2.

We note, as did Rose, 1987, that

$$F_n(ka; a_n; \lambda) = \begin{cases} a_F(a_n; \lambda) - b_F(a_n; \lambda)ka + c_F(a_n; \lambda)(ka)^2, & ka \to 0 \\ d_F(a_n; \lambda)/\sqrt{ka}, & ka \to \infty \end{cases} \tag{4.1}$$

so that an appropriate interpolation formula is

$$F_n^{\text{int}}(ka; a_n; \lambda) = \sqrt{\frac{s_F + p_F ka}{1 + q_F ka + r_F (ka)^2}}. \tag{4.2}$$

where the $(a_n; \lambda)$ dependences of the parameters have been omitted for brevity. On comparing the small and large ka expansions of this with the previous equation, the four parameters p_F to s_F can be found in terms of a_F to d_F. These are

$$\begin{aligned} s_F &= a_F^2 & r_F &= \frac{2s_F c_F - 3a_F b_F^2}{2b_F d_F^2 - a_F s_F} \\ p_F &= d_F^2 r_F & q_F &= \frac{2a_F b_F + p_F}{s_F}. \end{aligned} \tag{4.3}$$

From equation (3.2),

$$d_F = \frac{1}{\sqrt{\pi}}\left(1 + \frac{1}{2}(1+\lambda)(1-a_n)^2 + \frac{3}{2}(1-\lambda)(1-a_n)^4\right) \tag{4.4}$$

for both hole geometries. The p_F to s_F parameters are presented in fig. 16 for both hole cases and uniaxial as well as biaxial loading.

5 ASYMPTOTIC LIMITS FOR CRACK MOUTH OPENINGS

A number of asymptotic limits may be examined for the crack mouth openings, the normalized form of which were given in equation (2.69). These are similar to those for K_{tip}, but not so extensive. They often require more extreme values of the parameters before becoming "good" approximations. Some difficulties, in addition to those noted by Rose, 1987, were experienced in fitting interpolation formulae to $V_n(ka; a_n; \lambda)$. These functions must therefore be used with some care.

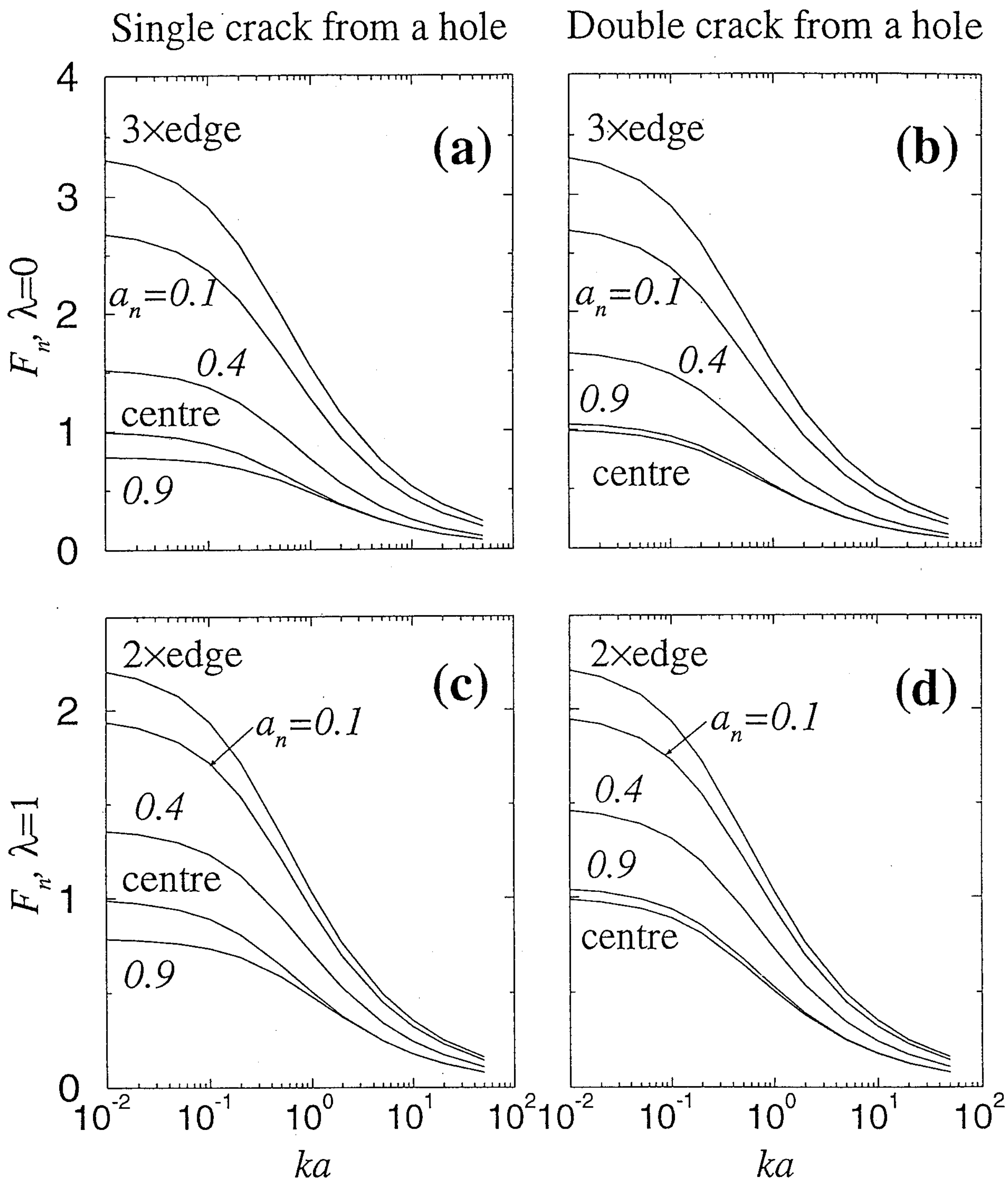

Figure 14: Representative plots of the $F_n(ka; a_n; \lambda)$ functions for $\lambda = 0$ and 1, for both hole cases and selected values of a_n.

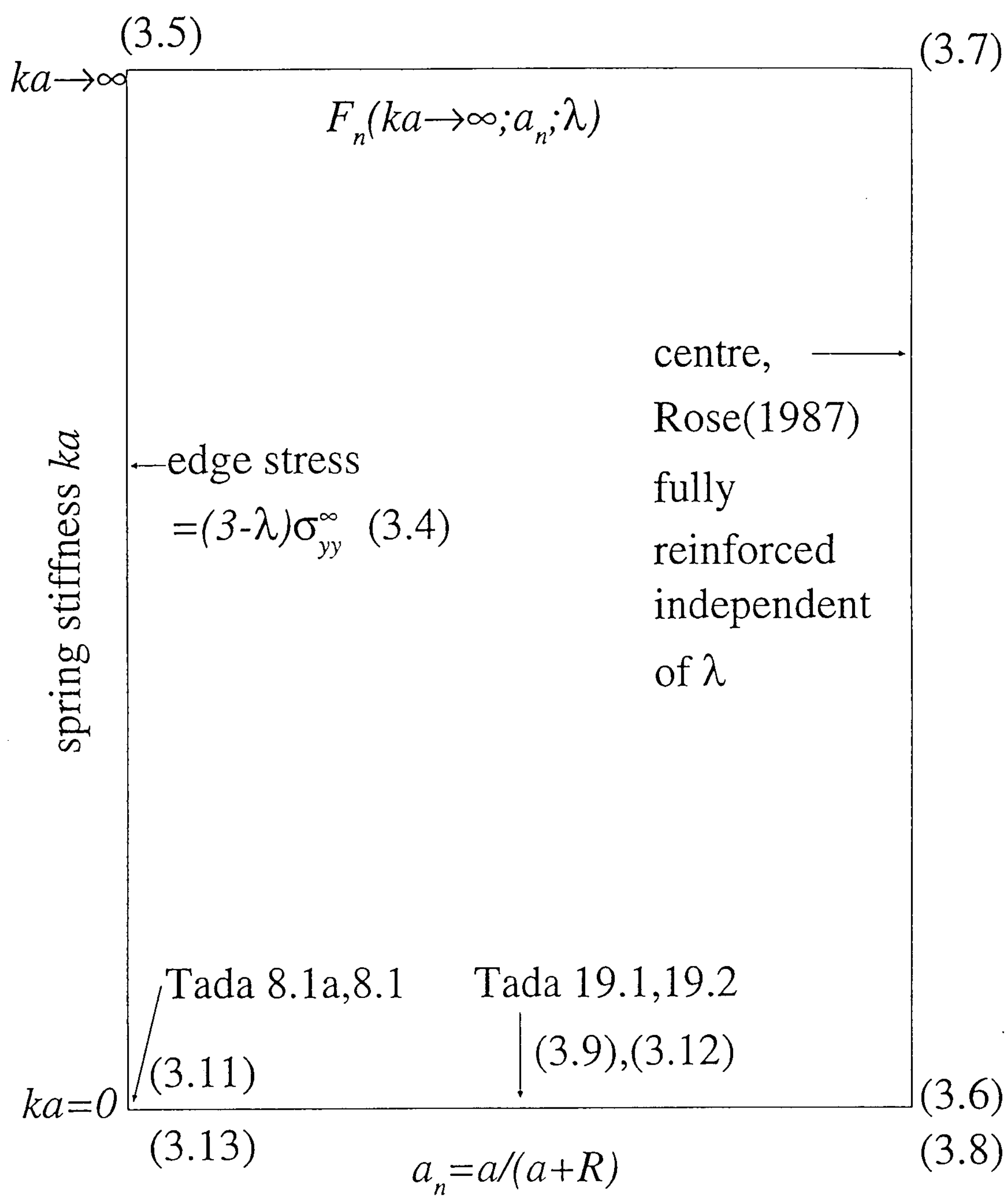

Figure 15: Diagram showing a "map" of the asymptotic limits to $F_n(ka; a_n; \lambda)$, and which equations these are.

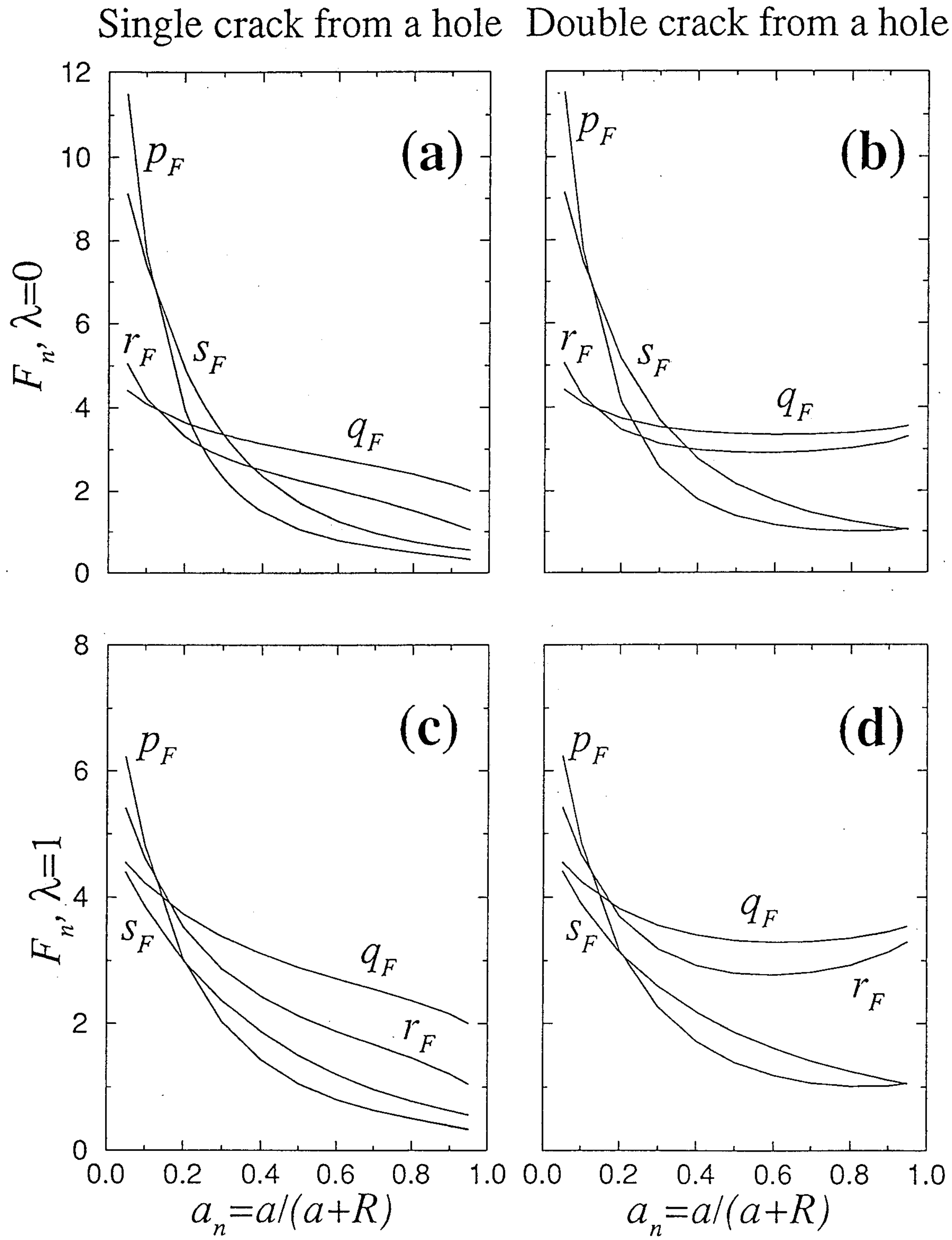

Figure 16: Parameters for the F_n interpolation formulae, equations (4.2).

5.1 Stiff Springs

In the limit of stiff springs, away from the crack tip, the crack opening becomes such that "the springs carry all the stress which would have existed if the crack were not there." This is another way of saying that K_{tip} is bounded with respect to increases in a by the reduction effected by the springs, equation (3.18).

Assuming large kl_n in equation (2.47), the second term dominates over the first. Using (2.1) in normalized form, we obtain

$$2\pi k l_n \delta_n(X) = -S_{yy}^{\infty\text{h}}(X). \tag{5.1}$$

$V_n(ka \to \infty; a_n; \lambda)$ is found for $X = B_l$ using (2.69), the second equation of (2.47) and (2.45), for both hole cases as

$$V_n(ka \to \infty; a_n; \lambda) \to \frac{1}{2}(3-\lambda)\frac{1}{ka}. \tag{5.2}$$

This limit requires k so large that even for small a, $ka \gg 1$. If a is too small, then the criterion stated earlier, "away from the crack tip", is not satisfied. In this case the material just beyond the crack tip will be carrying some of the stress that should be carried by the springs. These would thus not be extended as much as expected.

5.2 Large Hole or Short Crack: $a_n \to 0,\ ka = 0$

Both hole cases tend, in the $a_n \to 0$ limit with no springs, to an edge crack with an applied stress given by (3.3). From Tada *et al.*, 1985, page 8.1a,

$$V_n(0; 0; \lambda) = 1.454(3-\lambda),\ ka = 0. \tag{5.3}$$

5.3 Small R or Large a: $a_n \to 1$ with $ka = 0$

The asymptote in the limit of small holes, or long cracks, is not easy to determine because we are determining behaviour at the hole boundary. This is in contrast to the $F_n(ka; a_n \to 1; \lambda)$ limit where the hole, remote from the crack tip, became increasingly less significant as $a_n \to 1$.

The difficulty is best exhibited by the following considerations. Take a fixed hole size R, and a series of increasingly long cracks a. For stiff springs where $kR >> 1$ and $ka >> 1$, we should have the limit (5.2). In the case of no springs, as even weak springs will support any finite stress if the opening is wide enough, $\delta(R)$ would be expected to increase in proportion as a increases for the double crack case. For the single crack case, this will be reduced to a square root increase by the material on the other (uncracked) side of the hole. An approximation for both hole cases is to treat the hole as part of a centre crack as in fig. 7 (c) and (d). The profile of an unsprung centre crack was given in equation (3.19), from which $V_n(0; a_n \to 1; \lambda)$ is found by (2.69). Care is required with the change of variables in applying (3.19) to the correspondences of fig. 7 (c) and (d).

Taking the single crack case first, a becomes $(2R+a)/2$ and $x \mapsto x - a/2$. The opening is then calculated at $x = R$, $\delta(R) = \frac{4S_n S_y}{E'}\sqrt{2aR}$. This leads, as $a_n \to 1$, to

$$V_n(0; a_n \to 1; \lambda) \to \sqrt{2}\sqrt{\frac{1-a_n}{a_n}} \approx \sqrt{2(1-a_n)}\Big(1 + (1-a_n)/2 + \cdots\Big). \tag{5.4}$$

For the double crack, we use $a \mapsto a + R$ and x unchanged but set equal to R in (3.19), whereupon

$$V_n(0; a_n \to 1; \lambda) \to \sqrt{\frac{2-a_n}{a_n}} \approx 1 + (1-a_n) + (1-a_n)^2/2 + \cdots. \tag{5.5}$$

5.4 Large a with Springs

The previous section examined the large a or small R limit in the absence of springs, indicating different behaviour to that expected when finite stiffness springs are present. In this section, the integral equation (2.47) is re-examined under the transformations $X = 1/W$ and $B = 1/C$ as $B_r \to \infty$. In this case, the crack opening is no longer given by equation (2.49), but needs the additional term $\delta_n(\infty)$, the crack opening at infinity:

$$\delta_n(W) = \int_{C_r}^{W} D(C)\frac{\mathrm{d}C}{C^2} + \delta_n(\infty),\ \delta_n(\infty) = \frac{S_y}{2\pi k l_n}. \tag{5.6}$$

In this equation, $C_r = 1/B_r$. The integral equation to be solved then becomes, in the infinite crack limit ($C_r \to 0$),

$$\int_0^1 F(1/W, C)\frac{D(C)}{C^2}\mathrm{d}C - 2\pi k l_n \int_0^W \frac{D(C)}{C^2} = -S_y^{h\infty}(1/W), \tag{5.7}$$
$$S_y^{h\infty}(1/W) = \begin{cases} -S_y\left(\frac{1}{2}W^2 + \frac{3}{2}W^4\right), & \lambda = 0 \\ -S_y W^2, & \lambda = 1 \end{cases}.$$

It is not necessary to invoke the second change of variable $W = \sin(t)$ in this case, but we set $\overline{Q}(C) = D(C)/C^2$, and the crack mouth opening becomes

$$\delta_n(1) = \frac{S_y}{2\pi k l_n} + \int_0^1 \overline{Q}(C)\mathrm{d}C. \tag{5.8}$$

It is no longer possible to calculate a normalized crack mouth opening function V_n so comparisons with finite cracks will be made using $\delta_n(1)$. Similarly, the spring-stiffness will be expressed as kR rather than ka. Apart from these differences, numerical solution was similar to that described previously. The results are presented in appendix A.5 as tables of $\delta_n(1)$ against kR, calculated from above for the infinite crack cases, and from (2.47) for finite cracks. An interesting feature of these results is that, although the crack mouth opening becomes infinite for the infinite crack cases as $kR \to 0$, the difference $\delta_n(1) - \delta_n(\infty)$ remains finite.

Figure 17 shows how the crack profile near the crack mouth varies as the crack grows and becomes infinite for $kR = 1$ in the single crack, $\lambda = 0$ case.

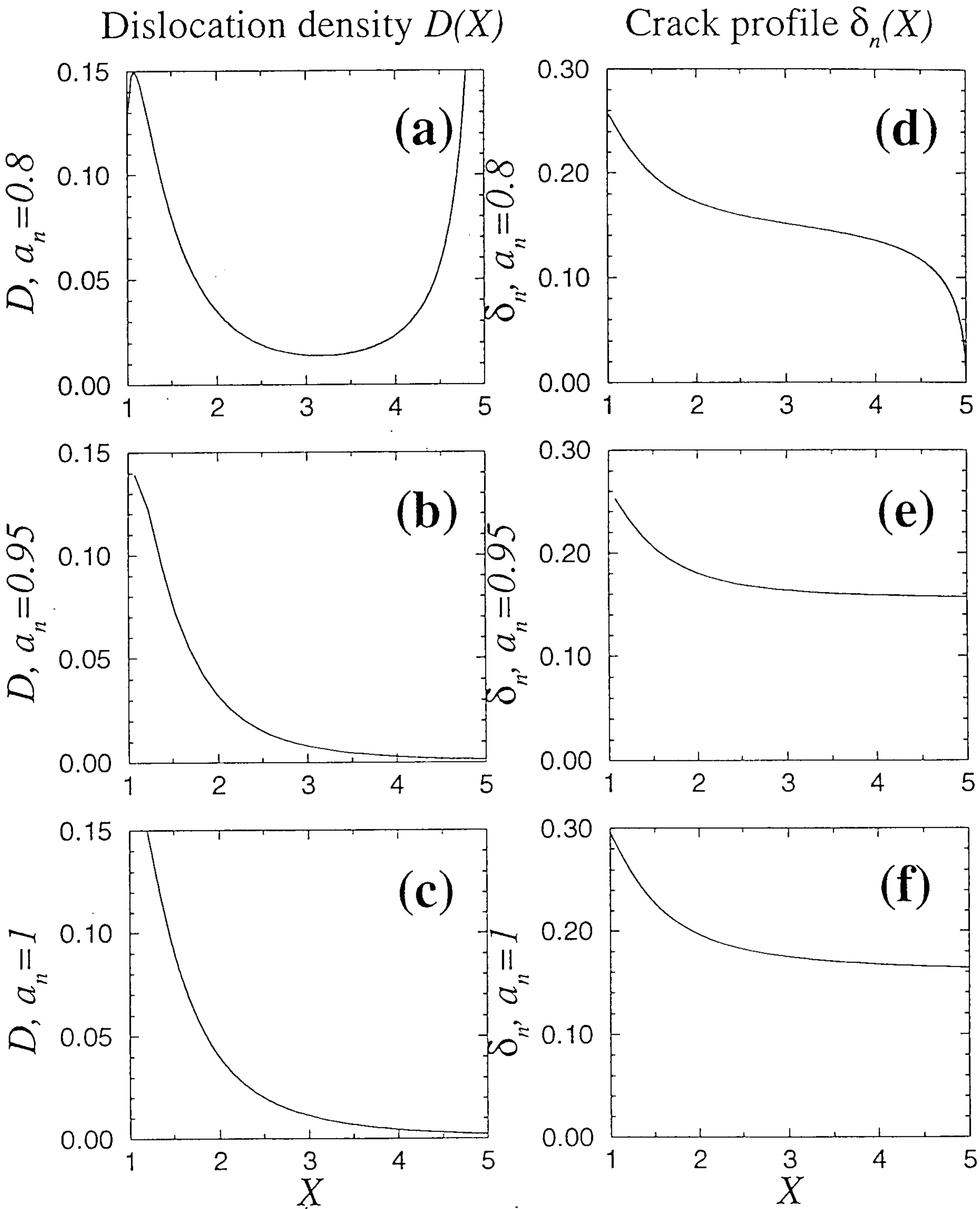

Figure 17: Near-mouth crack profiles for a single crack from a hole in uniaxial ($\lambda = 0$) tension for varying crack lengths and $kR = 1$. (a) to (c) show the dislocation density and (d) to (f) the near-mouth crack profile. The crack tips are at $X = 5, 20$, and ∞ for (d), (e) and (f) respectively.

5.5 Weak Springs, $ka \to 0$

In this limit, previous arguments for $K_{\rm tip}$ depended on the assumption that the crack profile for weak springs would be essentially the same as for no springs, but scaled down to produce $K_{\rm tip}$ instead of K_0, the stress intensity factor for no springs. In this approximation, the crack mouth opening $\delta(R)$ would become $\delta(R) = \delta_0(R)\frac{K_{\rm tip}}{K_0}$. This last factor was expanded as a series in ka, evaluated for the centre and edge cracks, with a similar expression expected for the hole cases. We assume therefore, that

$$V_n(ka \to 0; a_n; \lambda) \to a_V(a_n; \lambda) - b_V(a_n; \lambda)ka + c_V(a_n; \lambda)(ka)^2. \tag{5.9}$$

This is supported by noting that $D(B)$ in equation (2.47) may be expanded in powers of kl_n for ka so small that kR is too ($l_n = R$ for holes, a for edge and centre cracks):

$$D(B) = D^{(0)}(B) - kl_n D^{(1)}(B) + (kl_n)^2 D^{(2)}(B) - \cdots. \tag{5.10}$$

Insertion into (2.47) and examination of the powers of kl_n produces

$$(kl_n)^0 \ : \ \int_{B_l}^{B_r} F(X,B)D^{(0)}(B)\mathrm{d}B = -S_{yy}^{\infty\mathrm{h}}(X) \tag{5.11}$$

$$(kl_n)^1 \ : \ \int_{B_l}^{B_r} F(X,B)D^{(1)}(B)\mathrm{d}B = -2\pi\int_X^{B_r} D^{(0)}(B)\mathrm{d}B = -2\pi\delta_n^{(0)}(X).$$

The first of these is just the unsprung equation, whilst the second is the same equation but with a different "applied stress". It would thus have a similarly well-behaved solution, the first order dislocation density $D^{(1)}(B)$. Substituting (5.10) into the second equation of (2.49) will then produce a corrected crack mouth opening of the form of (5.9).

6 NUMERICAL RESULTS AND INTERPOLATION FORMULAE FOR V_n

Numerical values for $V_n(ka; a_n; \lambda)$ were calculated in a similar manner to those for $F_n(ka; a_n; \lambda)$. Asymptote (5.5) was excellent for $\lambda = 1$, but poor for $\lambda = 0$ as shown in table 4. Equation (5.4) required the second term to produce a satisfactory agreement for $\lambda = 1$, but was also poor for $\lambda = 0$.

For $a_n \to 0$, the predicted limit by (5.3) is $V_n = 2.908$ for $\lambda = 1$, and 4.362 for $\lambda = 0$. These are compared with calculated values in table 5.

Based on (5.2) and (5.9), a suitable interpolation function for $V_n(ka; a_n; \lambda)$ was chosen as

$$\begin{aligned} V_n^{\rm int}(ka; a_n; \lambda) &= \frac{s_V + p_V ka}{1 + q_V ka + r_V (ka)^2} = \frac{p_V(ka - z_0)}{r_V(ka - z_1)(ka - z_2)} \\ s_V = a_V \qquad & r_V = (b_V^2 - s_V c_V)/(s_V^2 - b_V d_V) \\ p_V = d_V r_V \qquad & q_V = (p_V + b_V)/s_V \\ & d_V = (3 - \lambda)/2. \end{aligned} \tag{6.1}$$

This produced good interpolations for most values of a_n and λ but, unlike equation (4.2) for $F_n(ka; a_n; \lambda)$, the denominator here had a root in the $ka > 0$ range for

Table 4: Testing the $V_n(0; a_n \to 1; \lambda)$ asymptotes, equations (5.4) and (5.5).

single crack from a hole				
a_n	$V_n(0;a_n;0)$	$V_n(0;a_n;1)$	1 term	2 term
0.7	1.1045	0.9502	0.775	0.891
0.8	0.8244	0.7354	0.632	0.696
0.9	0.5333	0.4954	0.447	0.470
0.95	0.3605	0.3434	0.316	0.324
0.98	0.2220	0.2164	0.200	0.202
double crack from a hole				
a_n	$V_n(0;a_n;0)$	$V_n(0;a_n;1)$	linear	quadratic
0.7	1.5138	1.3286	1.300	1.345
0.8	1.3222	1.2108	1.200	1.220
0.9	1.1516	1.1021	1.100	1.105
0.95	1.0728	1.0504	1.050	1.051
0.98	1.0267	1.0200	1.020	1.020

Table 5: Testing the $V_n(0; a_n \to 0; \lambda)$ asymptote, equation (5.3).

	single crack from a hole		double crack from a hole	
a_n	$V_n(0;a_n;0)$	$V_n(0;a_n;1)$	$V_n(0;a_n;0)$	$V_n(0;a_n;1)$
0.1	3.6077	2.5029	3.6292	2.5180
0.05	3.9559	2.6909	3.9619	2.6951
0.02	4.1834	2.8117	4.1845	2.8124
asymptote	4.362	2.908	4.362	2.908

Table 6: Testing the $V_n(ka \to \infty; a_n; \lambda)$ asymptote, equation (5.2). A few values of a_n have been included to show that the limit requires higher ka as a_n increases.

	asymptote		double crack from a hole			
ka	$\lambda=0$	$\lambda=1$	$V_n(ka;0.1;0)$	$V_n(ka;0.5;0)$	$V_n(ka;0.9;0)$	$V_n(ka;0.1;1)$
1	1.5	1.0	1.1196	0.7826	0.4681	0.7673
3	0.5	0.333	0.4560	0.3652	0.2318	0.3093
10	0.15	0.10	0.1463	0.1316	0.0944	0.0982
30	0.05	0.033	0.0496	0.0474	0.0386	0.0332

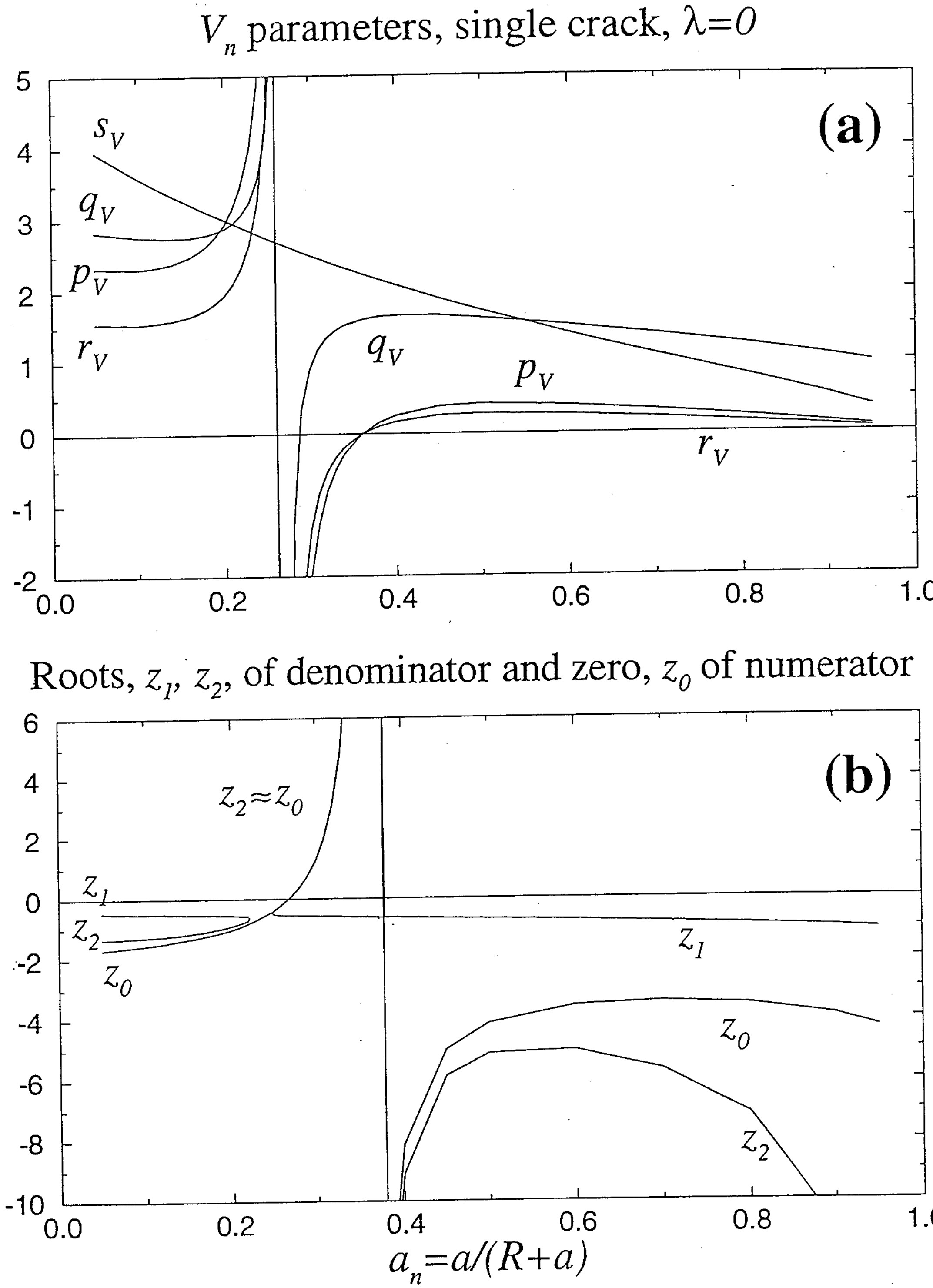

Figure 18: Showing (a) the parameters and (b) the zero z_0 and roots z_1, z_2 of the denominator of V_n^{int} as given by equation (6.1). These are against a_n for $\lambda = 0$ in the single crack from a hole case.

some a_n. This is shown in fig. 18(b) for the single crack from a hole case. In addition to this, the p_V, q_V and r_V parameters diverged as shown in fig. 18(a) at an a_n dependent on the hole case and λ.

In order to overcome these difficulties, two other interpolation formulae were examined. The first, more approximate one, was suggested by the near-coincidence of z_0 and z_2 (equation (6.1)) in the a_n range causing difficulty. This function contains only two parameters,

$$V_n^{\text{app}}(ka; a_n; \lambda) = \frac{d_V}{ka + (d_V/a_V)} \rightarrow \begin{cases} a_V, & ka \rightarrow 0 \\ d_V/ka, & ka \rightarrow \infty \end{cases} \tag{6.2}$$

which correctly matches the $ka = 0$ and $ka \rightarrow \infty$ limits.

An improvement is the three parameter "alternativee" function

$$\begin{aligned} V_n^{\text{alt}}(ka; a_n; \lambda) &= \sqrt{\frac{s_a}{1 + q_a ka + r_a (ka)^2}} = \sqrt{\frac{s_a/r_a}{(ka - r_1)(ka - r_2)}} \\ s_a = a_V^2 \qquad & r_a = (a_V/d_V)^2 \\ q_a = 2b_V/a_V \qquad & c_a = a_V(3q_a^2/4 - r_a)/2 \end{aligned} \tag{6.3}$$

which also matches the gradient $\frac{\partial V_n(ka; a_n; \lambda)}{\partial ka}$ as $ka \rightarrow 0$. It leads to the coefficient c_a for the $(ka)^2$ term, which may be compared to the true (numerically obtained) value c_V.

Given that b_V is obtained numerically, a preferred method of obtaining the three parameters was to fit to a_V, d_V and the value of V_n at an intermediate value of $ka = ka_0$. The parameters for this "new" function were:

$$\begin{aligned} s_n = a_V^2 \qquad & r_n = (a_V/d_V)^2 \\ v_n = V_n(ka_0; a_n; \lambda) \qquad & q_n = \frac{1}{ka_0}\left[\frac{s_n}{v_n^2} - (ka_0)^2 r_n - 1\right]. \end{aligned} \tag{6.4}$$

The parameters s_n, r_n, and q_n for $\lambda = 0$ and 1 for both hole cases are shown in fig. 19. These parameters vary smoothly with a_n, in contrast to those for V_n^{int}. The (denominator) roots r_1 and r_2 also cause no problem because they occur (when real) at negative ka only.

Comparisons between the various interpolation functions and the calculated values of $V_n(ka; a_n; \lambda)$ are presented in fig. 20 for the single crack case with $a_n = 0.9$, $\lambda = 0$. V_n^{int} is excellent for $ka < 2$ whilst V_n^{app} is in error by about 25%; too much to be useful. The situation is similar for $a_n = 0.5$, shown in fig. 21. The errors for all functions are reduced by a factor of about 5, and the alternatives to V_n^{int} are close enough to be considered useful.

When $a_n = 0.3$, the V_n^{int} function has a singularity in it, indicated in fig. 22 (a). It causes a divergence of the error for this function, shown in fig. 22 (b). In this case, the V_n^{alt} and V_n^{new} functions are actually more accurate than V_n^{int}. V_n^{int} possesses this singularity for a_n in the approximate range $0.26 \leq a_n \leq 0.37$.

Single crack from a hole Double crack from a hole

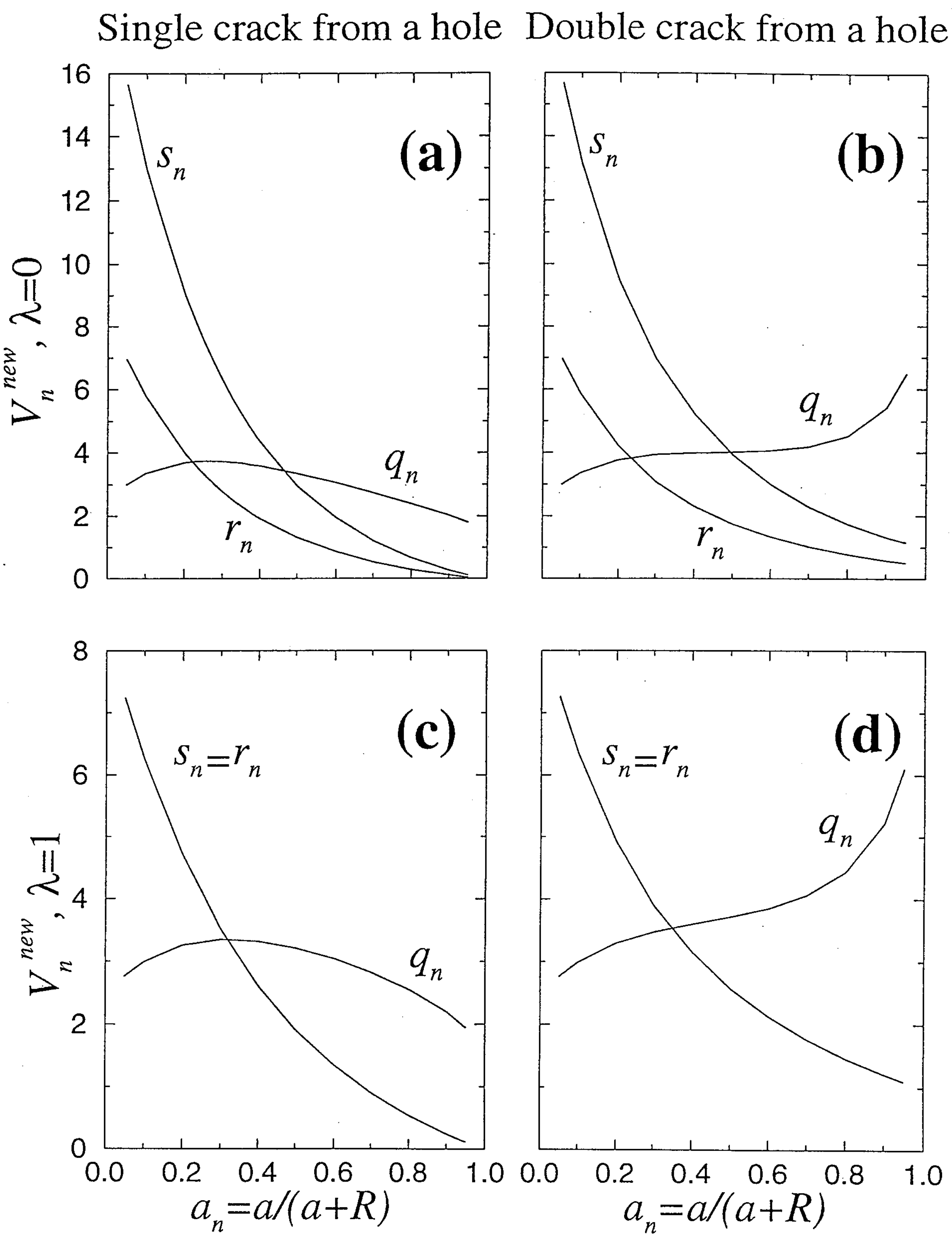

Figure 19: Plot of the parameters for V_n^{new}, equation (6.4), against a_n with $\lambda = 0$ for both hole cases.

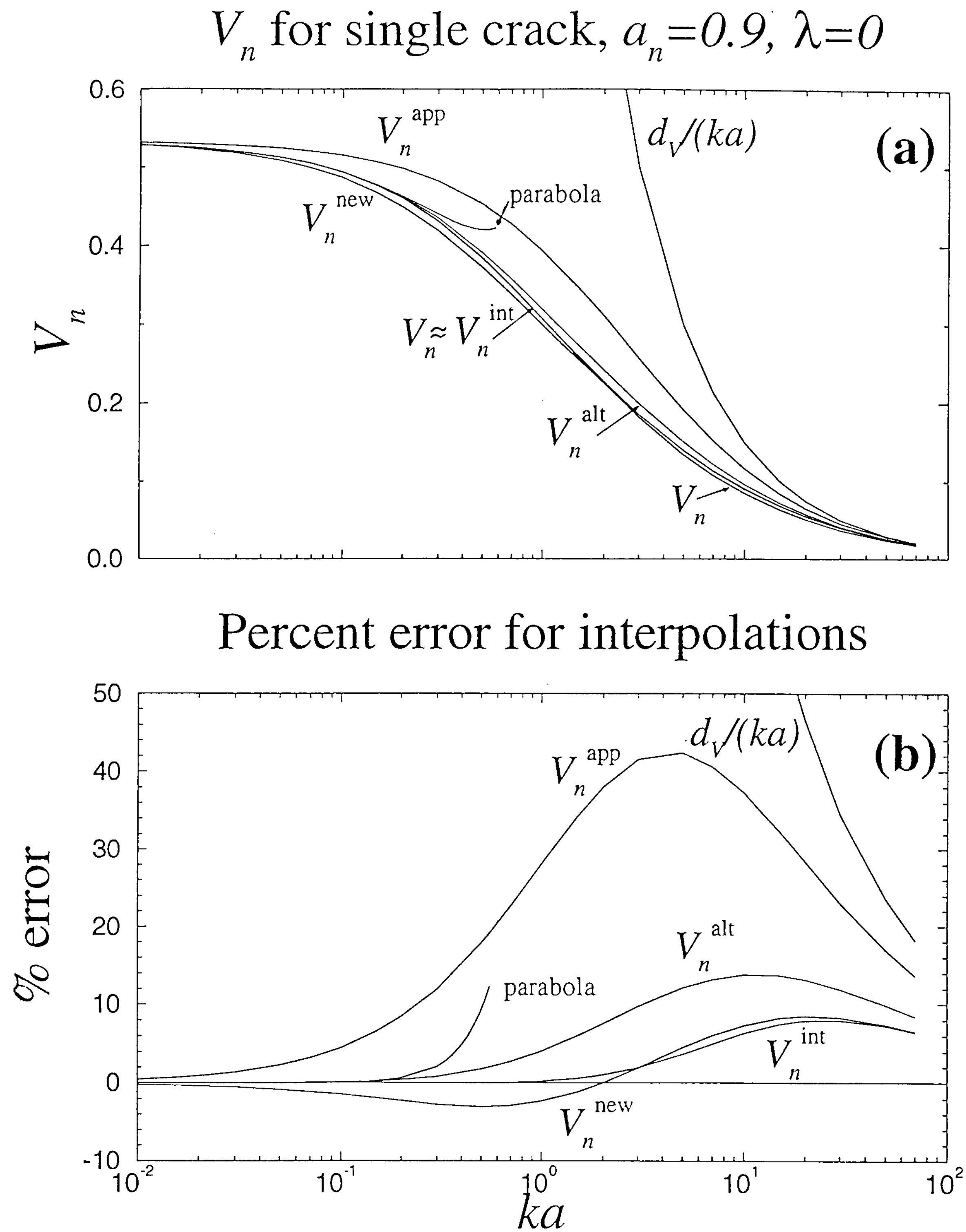

Figure 20: Comparison of the accuracy of the various V_n interpolating functions for $a_n = 0.9$. The small ka parabola and large ka, $d_V/(ka)$ limits are included.

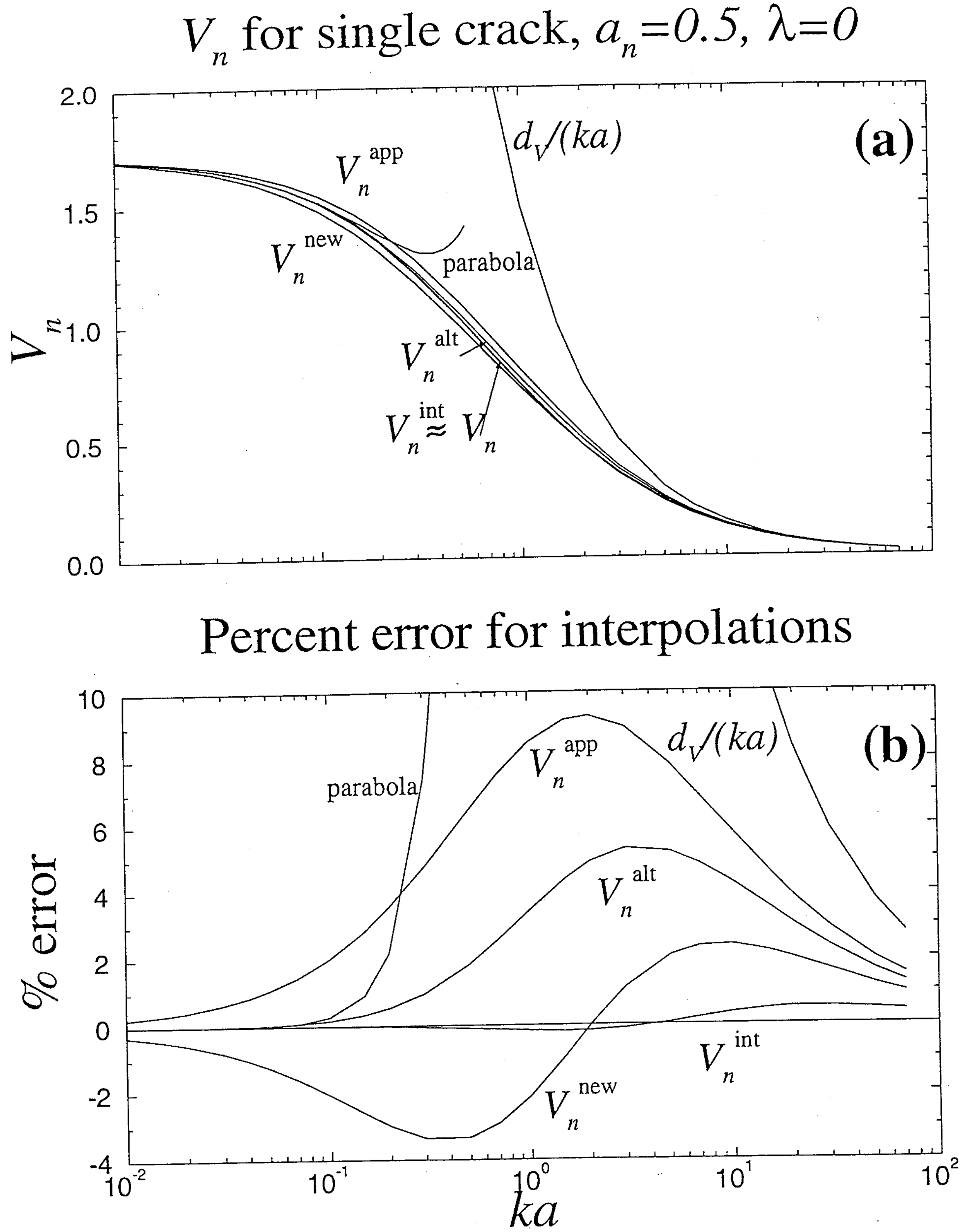

Figure 21: Comparison of the accuracy of the various V_n interpolating functions for $a_n = 0.5$. Note the overall reduction in error compared to fig. 20.

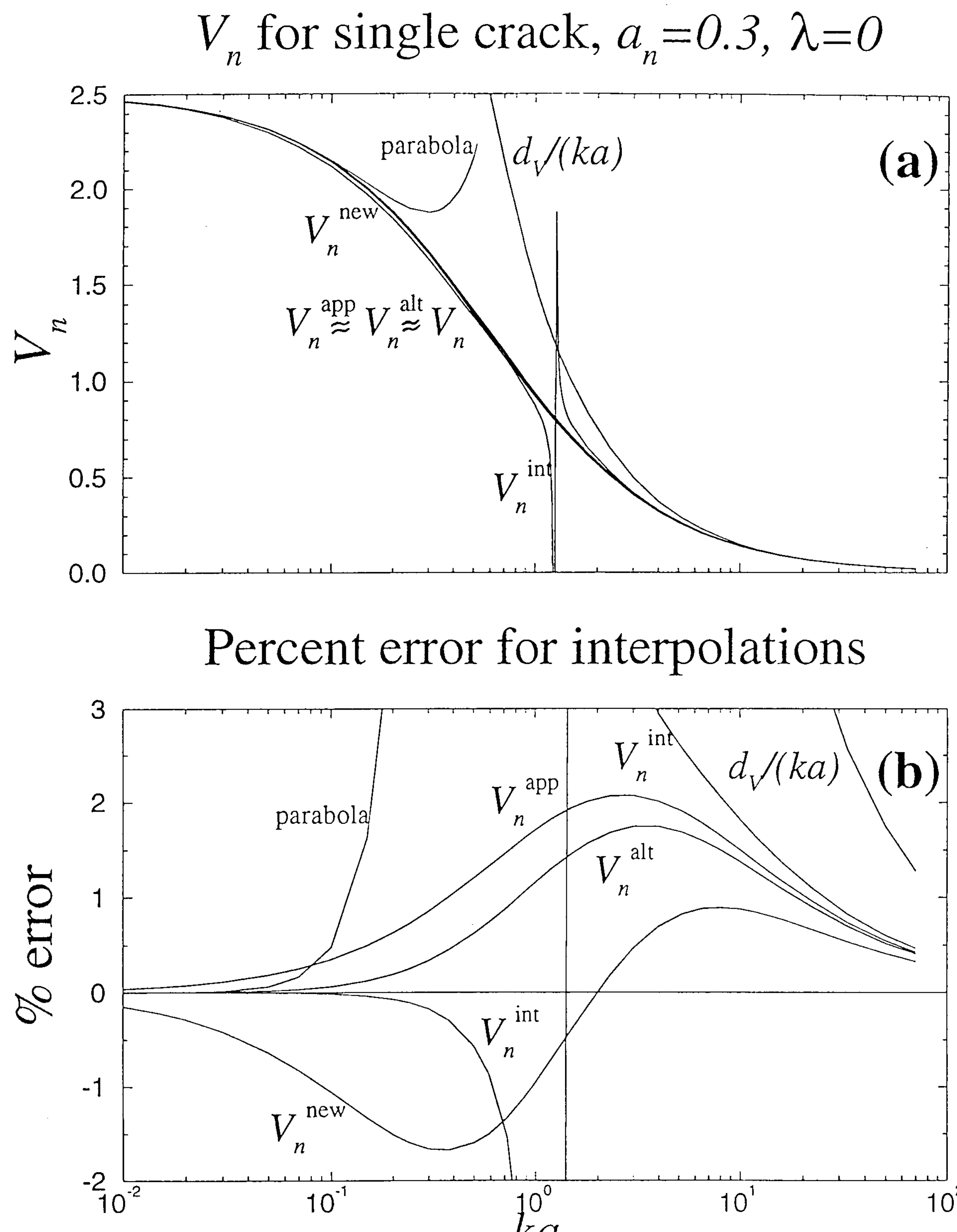

Figure 22: Comparison of the various V_n interpolating functions and their accuracy for $a_n = 0.3$. In this case, V_n^{int} has a singularity at $ka = 1.13$ so is not the preferred choice.

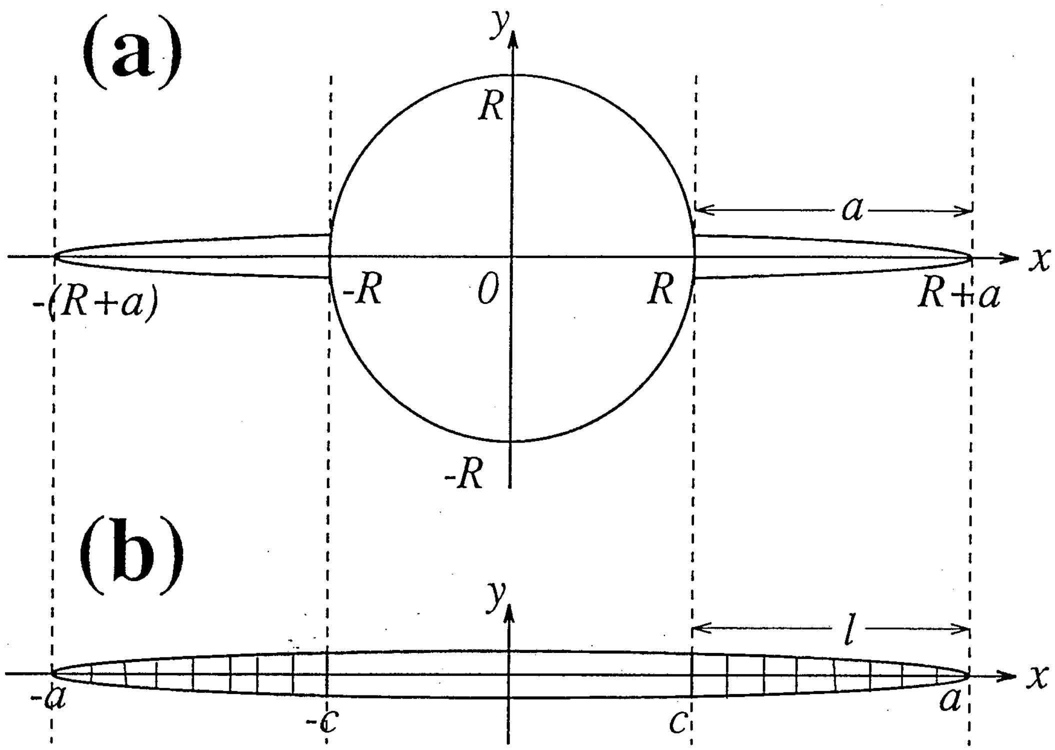

Figure 23: The symmetric double crack case (a) compared to the partially bridged centre crack (b) of Rose, 1987. The variables in (b) are those used by Rose, 1987.

7 COMPARISON OF K_{tip} FOR THE SYMMETRICALLY CRACKED HOLE AND THE PARTIALLY-BRIDGED CENTRE CRACK

An interesting comparison exists between K_{tip} for the symmetrically (double) cracked hole and partially bridged centre crack cases. In particular, the question of which has a lower K_{tip} arises, and thus whether drilling out the unbridged portion of the centre crack may be advantageous.

Figure 23 shows the variables used here (equation 2.68), and those used by Rose, 1987 for the partially bridged crack, his equations 15 (a) and (b). Care is required in the comparison, for Rose, 1987 normalizes K_{tip} based on a in fig. 24 (b), equivalent to $R+a$ in (24) (a). This means that the $F_n(ka; a_n; 0)$ function of equation (2.68) must be multiplied by $\sqrt{a/(R+a)} = \sqrt{a_n}$ before comparison. In addition, c/a is equivalent to $1 - a_n$.

For no springs, Rose, 1987 has the function $F(0, c/a) = 1$, whilst the function here will be $\sqrt{a_n}F_n(0; a_n; 0) = \sqrt{a_n}a_F(a_n; 0)$ from equation 4.1. These are compared in fig. 24 (a). The hole case has a lower K_{tip} for $c/a > 0.82$, or $a_n < 0.18$.

For stiff springs, Rose, 1987, equations 58 (b) and 24 indicate that $\sqrt{C}$ from

$$F(kl; c/a) = \sqrt{C}/\sqrt{kl},\ \sqrt{C} = \frac{1/\sqrt{\pi}}{\sqrt{1 + c/a}} \tag{7.1}$$

should be compared with $\sqrt{a_n}d_F$ from (4.1). This is done in fig. 24 (b) where, again as $c/a \to 1$, the hole case becomes more favourable with a lower K_{tip}. It is thus better (if lowering K_{tip} is desirable) to drill out the unbridged portion when a crack is bridged near the tips only.

In fig. 25, the value of a_n which makes K_{tip} equal in the two cases is plotted as a function of the spring stiffness ka (kl).

8 CONCLUSIONS

Values of normalized crack tip stress intensity factor from equation (2.68), and normalized crack mouth opening (2.69), along the lines of Rose, 1987 have been presented. These are for the cases of a single crack or symmetric double cracks emanating from a hole in an infinite plate. Both uniaxial and biaxial uniform remote tensions were treated.

Interpolation functions with respect to spring stiffness have been provided wherein the function parameters depend on the crack length relative to hole radius, a_n, and the biaxiality λ of the remote loading.

Difficulties were experienced with the interpolations for crack mouth opening for some values of a_n. In these cases, an alternative function avoided the problem, but this function was less accurate away from these a_n values.

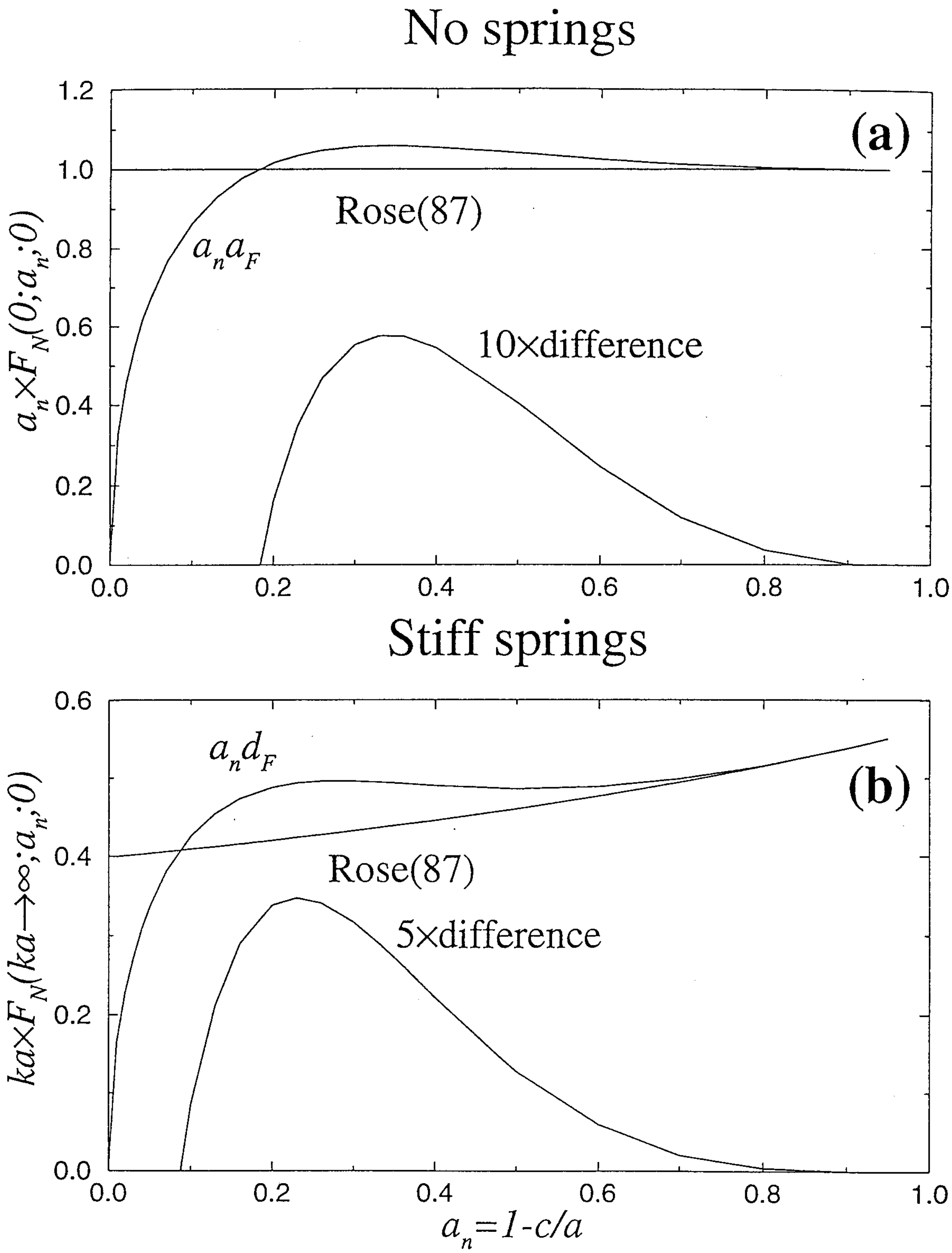

Figure 24: Comparison of normalized $K_{\rm tip}$ values for the symmetric double crack hole case, and the partially bridged centre crack. (a) is for no springs and (b) for stiff springs.

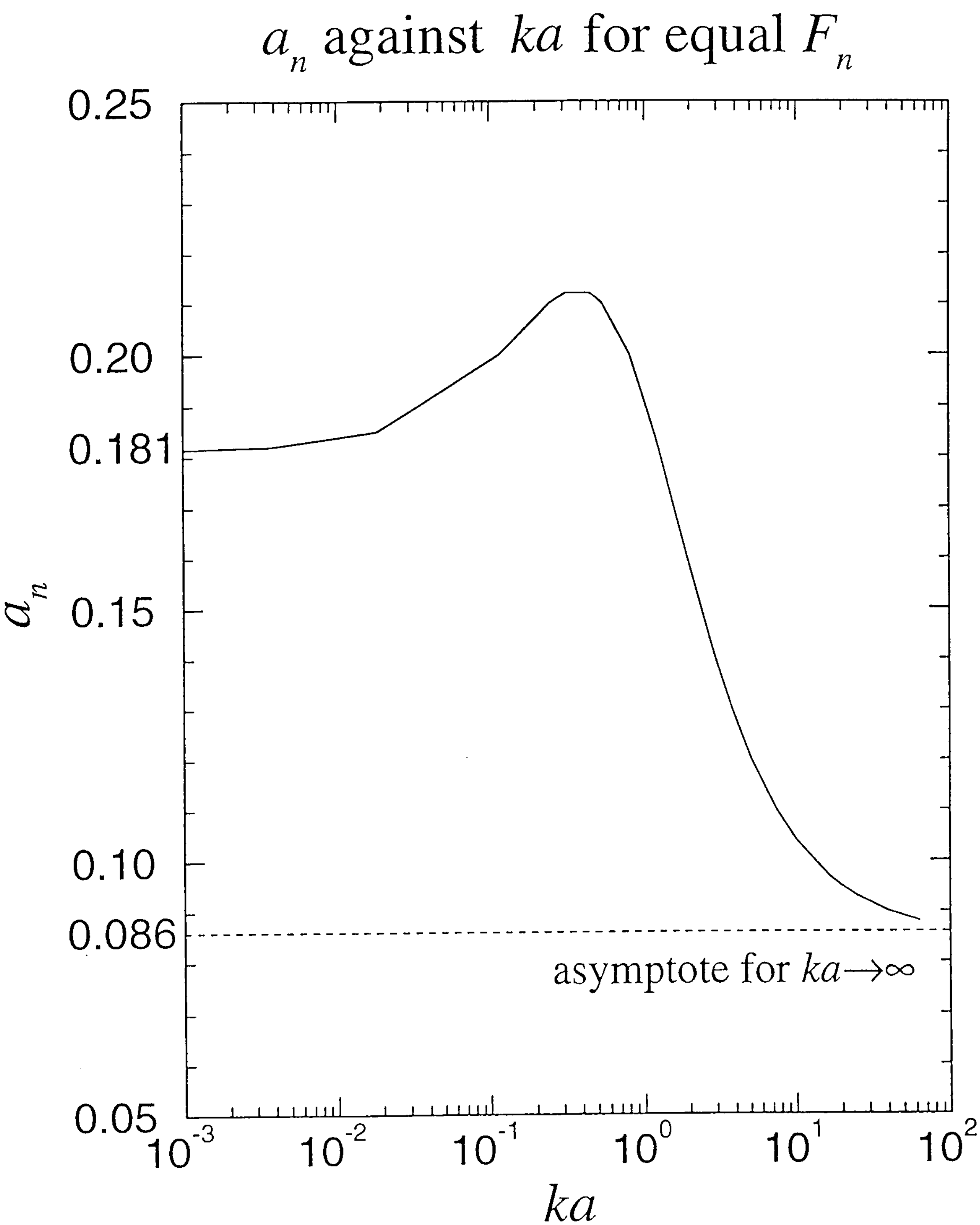

Figure 25: Values of $a_n = 1 - c/a$ which produce the same K_{tip} for the double crack hole and partially bridged centre crack cases, as a function of the spring stiffness.

9 REFERENCES

References

Bilby, B.A. and Eshelby, J.D. (1968), Dislocations and the Theory of Fracture., in *Fracture, An Advanced Treatise*, edited by Liebowitz, H., volume 1, chapter 2, Academic Press, New York.

List, R.D. (1969), A Two Dimensional Circular Inclusion Problem., *Proc.Comb.Phil.Soc.* **65**, 823–30.

Muskhelishvili, N.I (1953), *Some Basic Problems of the Mathematical Theory of Elasticity.*, Noordhoff, Groningen, Holland, The standard text on complex theory of elasticity.

Rose, L.R.F. (1987), Crack Reinforcement by Distributed Springs., *J.Mech.Phys.Sol.* **35**, 383–405.

Tada, H., Paris, P.C., and Irwin, G.R. (1985), *Stress Analysis of Cracks Handbook.*, Del Research Corporation, St. Louis, Missouri., The standard reference for crack problems.

A TABLES OF VALUES

Here are tabulated the various numerical results which are provided for completeness and reference purposes. The tables may be used as a more direct but less accurate method of obtaining $F_n(ka; a_n; \lambda)$ and $V_n(ka; a_n; \lambda)$ by looking up the values for a_n and ka closest to those needed.

A.1 $F_n(ka; a_n; \lambda)$

All values of $F_n(ka; a_n; \lambda)$ presented here are calculated using $n = 200$ points except for the few values for case (1,0) indicated by `# n=100`.

`# fnkan cases here`

`# case= edge, 3*edge, centre`

an\ka	.01	.02	.05	.10	.20	.50	1.00	2.00	5.00	10.00	20.00	50.00
edge	1.1029	1.0856	1.0377	.9690	.8622	.6705	.5166	.3821	.2482	.1771	.1258	.0799
3*edge	3.3087	3.2568	3.1131	2.9070	2.5866	2.0115	1.5498	1.1463	.7446	.5313	.3774	.2397
centre	.9875	.9754	.9412	.8907	.8083	.6483	.5088	.3801	.2480	.1770	.1258	.0799

`# case= (1,0)`

an\ka	.01	.02	.05	.10	.20	.50	1.00	2.00	5.00	10.00	20.00	50.00
.05	2.9732	2.9283	2.8033	2.6231	2.3399	1.8241	1.4046	1.0356	.6693	.4760	.3374	.2138
.10	2.6785	2.6393	2.5301	2.3717	2.1207	1.6571	1.2753	.9376	.6030	.4276	.3025	.1914
.20	2.1901	2.1600	2.0757	1.9522	1.7532	1.3767	1.0590	.7751	.4945	.3490	.2461	.1553
.40	1.5177	1.4993	1.4472	1.3696	1.2413	.9875	.7636	.5583	.3542	.2490	.1752	.1105
.60	1.1150	1.1034	1.0702	1.0199	.9350	.7598	.5975	.4427	.2840	.2008	.1418	.0897
.80	.8699	.8624	.8411	.8084	.7516	.6292	.5085	.3863	.2538	.1812	.1287	.0817
.90	.7810	.7751	.7583	.7322	.6864	.5847	.4804	.3706	.2467	.1772	.1262	.0802
.95	.7412	.7361	.7213	.6983	.6575	.5654	.4688	.3647	.2445	.1760	.1256	.0799

`# n= 100`

an\ka	.01	.02	.05	.10	.20	.50	1.00	2.00	5.00	10.00	20.00	50.00
.10	2.6769	2.6378	2.5289	2.3708	2.1201	1.6570	1.2755	.9379	.6035	.4282	.3032	.1923
.40	1.5171	1.4987	1.4467	1.3692	1.2410	.9875	.7637	.5585	.3544	.2494	.1757	.1110
.60	1.1147	1.1031	1.0699	1.0197	.9348	.7598	.5975	.4428	.2843	.2011	.1422	.0901
.90	.7810	.7752	.7583	.7323	.6865	.5847	.4805	.3708	.2470	.1775	.1266	.0807

`# case= (1,1)`

an\ka	.01	.02	.05	.10	.20	.50	1.00	2.00	5.00	10.00	20.00	50.00
.05	2.0645	2.0337	1.9479	1.8243	1.6298	1.2749	.9853	.7294	.4735	.3375	.2396	.1520
.10	1.9362	1.9085	1.8314	1.7195	1.5419	1.2127	.9398	.6963	.4516	.3217	.2282	.1447
.20	1.7110	1.6886	1.6255	1.5329	1.3834	1.0986	.8557	.6348	.4112	.2924	.2072	.1313
.40	1.3553	1.3399	1.2962	1.2309	1.1226	.9064	.7125	.5303	.3430	.2434	.1722	.1090
.60	1.0863	1.0755	1.0446	.9979	.9187	.7542	.5996	.4495	.2918	.2073	.1468	.0929
.80	.8747	.8673	.8462	.8137	.7574	.6355	.5148	.3921	.2580	.1844	.1310	.0831
.90	.7846	.7788	.7619	.7357	.6898	.5877	.4829	.3726	.2480	.1781	.1268	.0806
.95	.7428	.7377	.7228	.6998	.6589	.5666	.4697	.3653	.2449	.1763	.1257	.0800

`# case= (2,0)`

an\ka	.01	.02	.05	.10	.20	.50	1.00	2.00	5.00	10.00	20.00	50.00
.05	2.9777	2.9326	2.8072	2.6264	2.3424	1.8255	1.4053	1.0360	.6694	.4760	.3374	.2138
.10	2.6942	2.6545	2.5439	2.3836	2.1297	1.6621	1.2778	.9388	.6034	.4277	.3025	.1914
.20	2.2394	2.2078	2.1193	1.9899	1.7825	1.3930	1.0675	.7789	.4956	.3494	.2462	.1554
.40	1.6444	1.6223	1.5602	1.4684	1.3190	1.0317	.7866	.5684	.3570	.2501	.1756	.1106
.60	1.3054	1.2885	1.2408	1.1699	1.0537	.8276	.6325	.4577	.2882	.2023	.1424	.0898
.80	1.1080	1.0941	1.0549	.9967	.9011	.7143	.5519	.4045	.2586	.1829	.1293	.0819
.90	1.0411	1.0282	.9919	.9380	.8497	.6774	.5273	.3899	.2517	.1789	.1268	.0804
.95	1.0128	1.0004	.9652	.9132	.8279	.6620	.5173	.3844	.2495	.1777	.1261	.0800

`# case= (2,1)`

an\ka	.01	.02	.05	.10	.20	.50	1.00	2.00	5.00	10.00	20.00	50.00
.05	2.0676	2.0366	1.9506	1.8265	1.6315	1.2758	.9858	.7296	.4735	.3375	.2396	.1520
.10	1.9472	1.9192	1.8411	1.7278	1.5482	1.2162	.9416	.6971	.4519	.3218	.2283	.1447
.20	1.7477	1.7240	1.6578	1.5609	1.4051	1.1108	.8620	.6376	.4120	.2927	.2073	.1313
.40	1.4590	1.4405	1.3886	1.3117	1.1862	.9425	.7312	.5385	.3453	.2443	.1725	.1091
.60	1.2561	1.2405	1.1967	1.1315	1.0244	.8143	.6306	.4627	.2954	.2086	.1472	.0930
.80	1.1028	1.0892	1.0508	.9939	.9002	.7166	.5561	.4093	.2626	.1860	.1315	.0833
.90	1.0408	1.0280	.9918	.9382	.8504	.6787	.5288	.3914	.2529	.1797	.1274	.0808
.95	1.0131	1.0006	.9655	.9135	.8284	.6625	.5178	.3849	.2498	.1779	.1263	.0801

A.2 Parameters for F_n interpolations

Below are tabulated the parameters for $F_n(ka; a_n; \lambda)$ from equation 4.2. These are p_F to s_F together with the roots z_1, z_2 of the denominator and zero z_0 of the numerator. Complex roots are indicated by $z_1 = z_2 = 0$.

```
# Fnint cases here
# case= (1,0)
#  an      s         r         p          q          z1       z2      zero
  .05   9.120823  5.048863 11.482718  4.423212   .0000    .0000   -.7943
  .10   7.393766  4.228707  7.683244  4.090889   .0000    .0000   -.9623
  .20   4.933661  3.320904  3.955478  3.654874  -.5092   -.5914  -1.2473
  .21   4.743758  3.259147  3.730515  3.621078  -.5133   -.5977  -1.2716
  .22   4.562223  3.200843  3.522672  3.588530  -.5180   -.6031  -1.2951
  .23   4.388668  3.145690  3.330386  3.557139  -.5232   -.6076  -1.3178
  .24   4.222724  3.093417  3.152261  3.526824  -.5289   -.6112  -1.3396
  .25   4.064039  3.043781  2.987054  3.497509  -.5352   -.6139  -1.3606
  .26   3.912280  2.996563  2.833648  3.469125  -.5421   -.6156  -1.3807
  .27   3.767128  2.951563  2.691041  3.441608  -.5498   -.6162  -1.3999
  .28   3.628280  2.908600  2.558333  3.414902  -.5587   -.6154  -1.4182
  .29   3.495447  2.867509  2.434709  3.388953  -.5696   -.6123  -1.4357
  .30   3.368355  2.828141  2.319436  3.363711  -.5868   -.6026  -1.4522
  .31   3.246740  2.790357  2.211847  3.339131   .0000    .0000  -1.4679
  .32   3.130354  2.754032  2.111340  3.315170   .0000    .0000  -1.4826
  .33   3.018958  2.719050  2.017364  3.291789   .0000    .0000  -1.4965
  .34   2.912326  2.685305  1.929421  3.268952   .0000    .0000  -1.5094
  .35   2.810242  2.652698  1.847055  3.246622   .0000    .0000  -1.5215
  .36   2.712499  2.621139  1.769849  3.224769   .0000    .0000  -1.5326
  .37   2.618900  2.590544  1.697423  3.203361   .0000    .0000  -1.5429
  .38   2.529259  2.560834  1.629428  3.182371   .0000    .0000  -1.5522
  .39   2.443397  2.531938  1.565544  3.161770   .0000    .0000  -1.5607
  .40   2.361143  2.503788  1.505477  3.141533   .0000    .0000  -1.5684
  .50   1.704741  2.251269  1.064405  2.954300   .0000    .0000  -1.6016
  .60   1.270007  2.023035   .805467  2.781570   .0000    .0000  -1.5767
  .70    .975656  1.789572   .636609  2.606221   .0000    .0000  -1.5326
  .80    .769922  1.527659   .508298  2.408181   .0000    .0000  -1.5147
  .90    .619217  1.219432   .392165  2.159898   .0000    .0000  -1.5790
  .95    .557087  1.046475   .333943  2.005735   .0000    .0000  -1.6682
# n= 100 below
#  an      s         r         p          q          z1       z2      zero
  .10   7.384899  4.209123  7.647661  4.082275   .0000    .0000   -.9656
  .50   1.703599  2.245012  1.061446  2.951274   .0000    .0000  -1.6050
  .90    .619314  1.215541   .390914  2.157939   .0000    .0000  -1.5843
```

```
# case= (1,1)
# an     s          r          p          q          z1      z2      zero
  .05  4.395849   5.406093   6.228493   4.542905   .0000   .0000   -.7058
  .10  3.860911   4.616570   4.814229   4.227434   .0000   .0000   -.8020
  .20  3.007906   3.541231   3.031741   3.740225   .0000   .0000   -.9921
  .30  2.368473   2.874534   2.031375   3.384819   .0000   .0000  -1.1659
  .40  1.880227   2.434853   1.433510   3.113904   .0000   .0000  -1.3116
  .50  1.501610   2.123572   1.056178   2.897284   .0000   .0000  -1.4217
  .60  1.204138   1.882849    .806458   2.713650   .0000   .0000  -1.4931
  .70   .967810   1.673547    .632909   2.544725   .0000   .0000  -1.5291
  .80   .778273   1.461311    .503106   2.368870   .0000   .0000  -1.5469
  .90   .625040   1.204982    .391267   2.149893   .0000   .0000  -1.5975
  .95   .559528   1.045490    .334456   2.004897   .0000   .0000  -1.6729
# case= (2,0)
# an     s          r          p          q          z1      z2      zero
  .05  9.148752   5.061794  11.512127   4.428970   .0000   .0000   -.7947
  .10  7.482468   4.277533   7.771956   4.114280   .0000   .0000   -.9628
  .20  5.162956   3.482781   4.148287   3.741105  -.5006  -.5736  -1.2446
  .30  3.711968   3.135514   2.571521   3.539054   .0000   .0000  -1.4435
  .40  2.779610   2.980795   1.792291   3.426222   .0000   .0000  -1.5509
  .50  2.165132   2.921711   1.381391   3.367258   .0000   .0000  -1.5674
  .60  1.750041   2.915672   1.160869   3.344799   .0000   .0000  -1.5075
  .70  1.462874   2.946630   1.048212   3.351640   .0000   .0000  -1.3956
  .80  1.259535   3.019998   1.004844   3.390039   .0000   .0000  -1.2535
  .90  1.111635   3.173657   1.020638   3.477592   .0000   .0000  -1.0892
  .95  1.052047   3.309617   1.056139   3.553635   .0000   .0000   -.9961
# case= (2,1)
# an     s          r          p          q          z1      z2      zero
  .05  4.409128   5.418157   6.242393   4.548142   .0000   .0000   -.7063
  .10  3.905996   4.663816   4.863497   4.249244   .0000   .0000   -.8031
  .20  3.140531   3.706863   3.173543   3.825469   .0000   .0000   -.9896
  .30  2.592679   3.192142   2.255822   3.563108   .0000   .0000  -1.1493
  .40  2.184530   2.922182   1.720423   3.406087   .0000   .0000  -1.2698
  .50  1.869219   2.797765   1.391494   3.321233   .0000   .0000  -1.3433
  .60  1.618146   2.768740   1.185901   3.289304   .0000   .0000  -1.3645
  .70  1.414148   2.812244   1.063545   3.300560   .0000   .0000  -1.3297
  .80  1.247149   2.926437   1.007525   3.354364   .0000   .0000  -1.2378
  .90  1.110828   3.136583   1.018473   3.463413   .0000   .0000  -1.0907
  .95  1.052559   3.297806   1.054980   3.549074   .0000   .0000   -.9977
```

A.3 $V_n(ka; a_n; \lambda)$

Below are presented the numerically obtained values of $V_n(ka; a_n; \lambda)$.

vnkan cases here

case= edge, 3*edge, centre

an\ka	.01	.02	.05	.10	.20	.50	1.00	2.00	5.00	10.00	20.00	50.00
edge	1.4153	1.3830	1.2941	1.1680	.9753	.6462	.4077	.2306	.0981	.0497	.0250	.0100
3*edge	4.2459	4.1490	3.8823	3.5040	2.9259	1.9386	1.2231	.6918	.2943	.1491	.0750	.0300
centre	.9823	.9652	.9171	.8466	.7331	.5205	.3485	.2081	.0932	.0483	.0246	.0099

case= (1,0)

an\ka	.01	.02	.05	.10	.20	.50	1.00	2.00	5.00	10.00	20.00	50.00
.05	3.8688	3.7853	3.5543	3.2243	2.7147	1.8273	1.1692	.6704	.2894	.1477	.0745	.0299
.10	3.5325	3.4602	3.2597	2.9712	2.5210	1.7227	1.1174	.6494	.2844	.1462	.0741	.0298
.20	2.9519	2.8976	2.7459	2.5249	2.1733	1.5284	1.0182	.6078	.2740	.1430	.0731	.0297
.40	2.0559	2.0252	1.9386	1.8097	1.5978	1.1846	.8306	.5230	.2507	.1353	.0708	.0292
.60	1.3818	1.3653	1.3179	1.2463	1.1252	.8757	.6456	.4297	.2208	.1243	.0671	.0285
.80	.8165	.8089	.7867	.7527	.6938	.5660	.4395	.3113	.1748	.1049	.0598	.0267
.90	.5289	.5246	.5123	.4931	.4593	.3843	.3072	.2260	.1349	.0853	.0512	.0243
.95	.3578	.3551	.3475	.3356	.3146	.2671	.2172	.1635	.1016	.0669	.0420	.0212

n= 100

an\ka	.01	.02	.05	.10	.20	.50	1.00	2.00	5.00	10.00	20.00	50.00
.10	3.5212	3.4493	3.2498	2.9627	2.5145	1.7192	1.1157	.6487	.2842	.1462	.0740	.0298
.40	2.0504	2.0199	1.9335	1.8051	1.5939	1.1818	.8288	.5220	.2503	.1351	.0707	.0292
.60	1.3789	1.3623	1.3151	1.2435	1.1226	.8736	.6439	.4285	.2202	.1241	.0670	.0284
.90	.5293	.5250	.5125	.4932	.4593	.3840	.3066	.2253	.1343	.0848	.0509	.0241

case= (1,1)

an\ka	.01	.02	.05	.10	.20	.50	1.00	2.00	5.00	10.00	20.00	50.00
.05	2.6314	2.5744	2.4167	2.1914	1.8435	1.2384	.7903	.4517	.1941	.0988	.0498	.0200
.10	2.4503	2.3997	2.2595	2.0578	1.7432	1.1864	.7657	.4422	.1920	.0982	.0496	.0199
.20	2.1268	2.0870	1.9758	1.8139	1.5567	1.0864	.7168	.4226	.1874	.0969	.0492	.0199
.40	1.5921	1.5674	1.4977	1.3942	1.2245	.8956	.6174	.3801	.1766	.0935	.0482	.0197
.60	1.1471	1.1325	1.0908	1.0279	.9219	.7053	.5087	.3288	.1617	.0884	.0467	.0194
.80	.7279	.7206	.6994	.6670	.6109	.4903	.3724	.2557	.1363	.0786	.0432	.0186
.90	.4911	.4869	.4747	.4557	.4226	.3490	.2740	.1961	.1114	.0675	.0388	.0175
.95	.3408	.3381	.3305	.3187	.2977	.2504	.2010	.1481	.0884	.0558	.0336	.0160

case= (2,0)

an\ka	.01	.02	.05	.10	.20	.50	1.00	2.00	5.00	10.00	20.00	50.00
.05	3.8745	3.7908	3.5592	3.2284	2.7176	1.8286	1.1697	.6706	.2894	.1477	.0745	.0299
.10	3.5531	3.4800	3.2773	2.9859	2.5317	1.7278	1.1196	.6502	.2846	.1463	.0741	.0299
.20	3.0188	2.9621	2.8038	2.5740	2.2099	1.5466	1.0264	.6107	.2747	.1432	.0732	.0297
.40	2.2443	2.2079	2.1053	1.9542	1.7094	1.2448	.8597	.5343	.2532	.1361	.0710	.0293
.60	1.7059	1.6807	1.6094	1.5037	1.3305	.9945	.7073	.4557	.2272	.1263	.0677	.0286
.80	1.3026	1.2837	1.2302	1.1510	1.0212	.7694	.5540	.3645	.1898	.1099	.0613	.0270
.90	1.1338	1.1166	1.0682	.9966	.8800	.6563	.4681	.3060	.1601	.0944	.0542	.0249
.95	1.0554	1.0387	.9915	.9220	.8093	.5952	.4178	.2680	.1375	.0809	.0470	.0223

case= (2,1)

an\ka	.01	.02	.05	.10	.20	.50	1.00	2.00	5.00	10.00	20.00	50.00
.05	2.6354	2.5782	2.4201	2.1942	1.8455	1.2393	.7907	.4518	.1942	.0988	.0498	.0200
.10	2.4648	2.4137	2.2719	2.0682	1.7508	1.1901	.7673	.4427	.1921	.0982	.0496	.0199
.20	2.1764	2.1348	2.0187	1.8503	1.5838	1.0999	.7229	.4248	.1879	.0970	.0492	.0199
.40	1.7462	1.7168	1.6341	1.5124	1.3158	.9448	.6411	.3894	.1787	.0941	.0484	.0197
.60	1.4359	1.4135	1.3504	1.2570	1.1045	.8107	.5633	.3516	.1673	.0901	.0471	.0195
.80	1.1921	1.1739	1.1226	1.0467	.9225	.6829	.4802	.3053	.1501	.0831	.0446	.0189
.90	1.0846	1.0676	1.0198	.9491	.8342	.6141	.4300	.2730	.1353	.0760	.0416	.0181
.95	1.0331	1.0164	.9694	.9001	.7878	.5747	.3985	.2504	.1230	.0692	.0383	.0170

A.4 V_n interpolation parameters

The s_n, r_n, q_n parameters from equation 6.4 are tabulated below with the roots z_1, z_2 of the denominator. Complex roots are again indicated by $z_1 = z_2 = 0$.

```
# Vnnew cases here
# Vnnew case=(1,0)
#  an       sn          rn         qn         z1        z2
  .05   15.649078   6.955146   2.998574    .0000     .0000
  .10   13.015436   5.784638   3.360938    .0000     .0000
  .20    9.049259   4.021893   3.705761    .0000     .0000
  .21    8.727861   3.879049   3.719977    .0000     .0000
  .22    8.417930   3.741302   3.731308    .0000     .0000
  .23    8.118999   3.608444   3.739917    .0000     .0000
  .24    7.830621   3.480276   3.745960   -.4903    -.5861
  .25    7.552372   3.356610   3.749582   -.4400    -.6770
  .26    7.283846   3.237265   3.750921   -.4159    -.7428
  .27    7.024656   3.122070   3.750108   -.3996    -.8016
  .28    6.774435   3.010860   3.747266   -.3875    -.8571
  .29    6.532829   2.903479   3.742512   -.3781    -.9109
  .30    6.299502   2.799779   3.735954   -.3706    -.9638
  .31    6.074134   2.699615   3.727697   -.3645   -1.0164
  .32    5.856417   2.602852   3.717838   -.3594   -1.0690
  .33    5.646058   2.509359   3.706472   -.3552   -1.1218
  .34    5.442778   2.419013   3.693684   -.3518   -1.1752
  .35    5.246309   2.331693   3.679557   -.3489   -1.2291
  .36    5.056393   2.247286   3.664171   -.3466   -1.2839
  .37    4.872787   2.165683   3.647598   -.3447   -1.3396
  .38    4.695256   2.086780   3.629908   -.3432   -1.3963
  .39    4.523574   2.010477   3.611168   -.3421   -1.4541
  .40    4.357527   1.936679   3.591439   -.3412   -1.5132
  .50    2.965678   1.318079   3.351233   -.3453   -2.1972
  .60    1.956834    .869704   3.059728   -.3646   -3.1535
  .70    1.219928    .542190   2.740393   -.3959   -4.6584
  .80     .679650    .302067   2.401634   -.4408   -7.5099
  .90     .284419    .126408   2.032365   -.5081  -15.5697
  .95     .129933    .057748   1.816074   -.5606  -30.8877
# n= 100
#  an       sn          rn         qn         z1        z2
  .10   12.931217   5.747208   3.368665    .0000     .0000
  .50    2.951357   1.311714   3.363324   -.3433   -2.2208
  .90     .284799    .126578   2.052668   -.5028  -15.7139
```

Vnnew case=(1,1)

# an	sn	rn	qn	z1	z2
.05	7.241101	7.241101	2.764161	.0000	.0000
.10	6.264352	6.264352	2.992208	.0000	.0000
.20	4.700724	4.700724	3.258106	.0000	.0000
.30	3.521932	3.521932	3.347423	.0000	.0000
.40	2.616385	2.616385	3.320101	-.4918	-.7772
.50	1.909595	1.909595	3.212369	-.4124	-1.2698
.60	1.350404	1.350404	3.045078	-.3990	-1.8559
.70	.902797	.902797	2.827394	-.4064	-2.7254
.80	.540847	.540847	2.555768	-.4305	-4.2950
.90	.245451	.245451	2.199782	-.4803	-8.4819
.95	.117948	.117948	1.951891	-.5292	-16.0195

Vnnew case= (2,0)

# an	sn	rn	qn	z1	z2
.05	15.696815	6.976362	2.998734	.0000	.0000
.10	13.170855	5.853713	3.369399	.0000	.0000
.20	9.472064	4.209806	3.777178	.0000	.0000
.30	6.965895	3.095953	3.938914	-.3504	-.9219
.40	5.207810	2.314582	3.990995	-.3042	-1.4200
.50	3.938549	1.750466	4.011750	-.2846	-2.0072
.60	2.999865	1.333273	4.057477	-.2705	-2.7727
.70	2.291505	1.018447	4.189919	-.2544	-3.8596
.80	1.748091	.776929	4.523079	-.2302	-5.5915
.90	1.326076	.589367	5.404253	-.1889	-8.9807
.95	1.150844	.511486	6.490885	-.1560	-12.5343

Vnnew case= (2,1)

# an	sn	rn	qn	z1	z2
.05	7.263342	7.263342	2.763266	.0000	.0000
.10	6.340202	6.340202	2.993940	.0000	.0000
.20	4.926668	4.926668	3.294619	.0000	.0000
.30	3.910764	3.910764	3.472497	.0000	.0000
.40	3.156499	3.156499	3.595992	-.4821	-.6571
.50	2.580335	2.580335	3.709645	-.3594	-1.0782
.60	2.128512	2.128512	3.850302	-.3143	-1.4946
.70	1.765214	1.765214	4.062959	-.2802	-2.0214
.80	1.466120	1.466120	4.433660	-.2455	-2.7786
.90	1.214711	1.214711	5.221419	-.2009	-4.0976
.95	1.103268	1.103268	6.094277	-.1693	-5.3546

A.5 Normalized crack-mouth openings $\delta_n(R)$ against kR

The following data were calculated for comparison with semi-infinite cracks from a circular hole. Here the length scale is R and not a, hence spring stiffness is kR. The rows with $a_n = 1.00$ were calculated for semi-infinite cracks in a different way to finite cracks from the hole. The row labelled **#dninf** indicates the opening at infinity for the semi-infinite crack cases.

```
# Normalized crack mouth openings, dn(1)= d(x=R)/ R, d= 2*u, against kR for semi-infinite
# crack from a hole limit.
# hole1, lbda= 0
# an\kr      .01     .02     .05     .10     .20     .50    1.00    2.00    5.00   10.00   20.00   50.00
   .05     .0662   .0661   .0659   .0655   .0647   .0626   .0592   .0535   .0413   .0297   .0189   .0088
   .10     .1273   .1270   .1261   .1246   .1218   .1141   .1031   .0862   .0575   .0366   .0210   .0091
   .20     .2382   .2371   .2338   .2285   .2185   .1931   .1616   .1216   .0694   .0402   .0218   .0092
   .40     .4385   .4341   .4214   .4018   .3678   .2935   .2200   .1472   .0747   .0414   .0220   .0092
   .60     .6558   .6441   .6116   .5646   .4902   .3543   .2458   .1552   .0758   .0416   .0220   .0092
   .80    1.0109   .9752   .8833   .7669   .6132   .3964   .2590   .1584   .0761   .0416   .0220   .0092
   .90    1.4231  1.3340  1.1308   .9155   .6817   .4123   .2628   .1590   .0761   .0415   .0220   .0092
   .95    1.9146  1.7166  1.3373  1.0121   .7159   .4179   .2635   .1586   .0756   .0412   .0217   .0090
   .98    2.6291  2.1694  1.5064  1.0690   .7275   .4133   .2570   .1525   .0710   .0380   .0197   .0080
  1.00   16.3292  8.3520  3.5397  1.9078  1.0620   .5100   .2961   .1700   .0786   .0423   .0222   .0092
#dninf   15.9154  7.9577  3.1831  1.5915   .7958   .3183   .1592   .0796   .0318   .0159   .0080   .0032
# hole1, lbda= 0, n= 100 only
# an\kr      .01     .02     .05     .10     .20     .50    1.00    2.00    5.00   10.00   20.00   50.00
   .05     .0660   .0659   .0657   .0653   .0645   .0624   .0590   .0533   .0412   .0297   .0188   .0088
   .80    1.0098   .9741   .8821   .7655   .6118   .3951   .2581   .1578   .0759   .0415   .0220   .0092
   .95    1.9163  1.7168  1.3349  1.0080   .7110   .4132   .2594   .1552   .0731   .0393   .0205   .0083
   .98    2.6315  2.1635  1.4897  1.0467   .7025   .3885   .2348   .1347   .0601   .0313   .0158   .0061
  1.00   16.3311  8.2455  3.4349  1.8082   .9716   .4378   .2407   .1311   .0572   .0298   .0153   .0063
# hole1, lbda= 1
# an\kr      .01     .02     .05     .10     .20     .50    1.00    2.00    5.00   10.00   20.00   50.00
   .05     .0450   .0450   .0448   .0446   .0440   .0425   .0403   .0364   .0280   .0202   .0127   .0059
   .10     .0883   .0881   .0875   .0865   .0845   .0791   .0714   .0596   .0396   .0251   .0143   .0061
   .20     .1717   .1709   .1684   .1645   .1572   .1386   .1156   .0864   .0486   .0278   .0149   .0062
   .40     .3396   .3361   .3259   .3102   .2828   .2235   .1653   .1085   .0533   .0289   .0151   .0062
   .60     .5442   .5339   .5054   .4641   .3992   .2821   .1905   .1165   .0545   .0291   .0152   .0062
   .80     .8993   .8653   .7779   .6677   .5239   .3255   .2046   .1201   .0550   .0292   .0152   .0062
   .90    1.3160  1.2283  1.0290   .8193   .5945   .3427   .2093   .1212   .0552   .0293   .0152   .0062
   .95    1.8124  1.6154  1.2392   .9189   .6312   .3499   .2111   .1216   .0552   .0292   .0151   .0062
   .98    2.5412  2.0818  1.4207   .9872   .6529   .3537   .2116   .1211   .0544   .0286   .0147   .0059
  1.00   16.2198  8.2441  3.4349  1.8084   .9717   .4380   .2408   .1312   .0572   .0299   .0153   .0063
# hole2, lbda= 0
# an\kr      .01     .02     .05     .10     .20     .50    1.00    2.00    5.00   10.00   20.00   50.00
   .05     .0663   .0662   .0660   .0656   .0648   .0627   .0593   .0536   .0414   .0298   .0189   .0088
   .10     .1281   .1277   .1268   .1254   .1225   .1147   .1036   .0866   .0577   .0367   .0210   .0091
   .20     .2437   .2425   .2391   .2335   .2231   .1967   .1642   .1231   .0698   .0404   .0219   .0092
   .40     .4789   .4737   .4586   .4355   .3958   .3110   .2297   .1515   .0758   .0417   .0221   .0092
   .60     .8085   .7908   .7423   .6740   .5704   .3941   .2639   .1621   .0773   .0420   .0222   .0092
   .80    1.5884  1.5041  1.3002  1.0659   .7925   .4642   .2857   .1675   .0780   .0421   .0222   .0092
   .90    2.8937  2.5811  1.9619  1.4206   .9393   .4958   .2936   .1692   .0782   .0421   .0221   .0092
   .95    4.9551  4.0218  2.6028  1.6787  1.0212   .5091   .2962   .1693   .0778   .0418   .0219   .0090
   .98    8.7106  6.0132  3.1843  1.8506  1.0594   .5075   .2900   .1631   .0731   .0385   .0198   .0081
# hole2, lbda= 1
# an\kr      .01     .02     .05     .10     .20     .50    1.00    2.00    5.00   10.00   20.00   50.00
   .05     .0451   .0450   .0449   .0446   .0441   .0426   .0403   .0364   .0281   .0202   .0128   .0059
   .10     .0888   .0886   .0880   .0870   .0850   .0795   .0717   .0599   .0397   .0251   .0143   .0061
   .20     .1758   .1749   .1724   .1683   .1606   .1413   .1175   .0875   .0490   .0280   .0150   .0062
   .40     .3727   .3685   .3563   .3377   .3057   .2378   .1732   .1120   .0542   .0292   .0152   .0062
   .60     .6802   .6645   .6217   .5614   .4704   .3172   .2065   .1225   .0559   .0295   .0153   .0062
   .80    1.4505  1.3697  1.1746   .9513   .6930   .3887   .2292   .1285   .0568   .0297   .0153   .0063
   .90    2.7572  2.4488  1.8394  1.3093   .8423   .4218   .2381   .1307   .0571   .0298   .0153   .0062
   .95    4.8247  3.8955  2.4854  1.5714   .9272   .4370   .2418   .1316   .0572   .0298   .0153   .0062
   .98    8.6047  5.9085  3.0844  1.7579   .9775   .4445   .2430   .1311   .0564   .0291   .0148   .0060
```

Stress Intensity Factors and Crack Mouth Openings for Bridged Cracks Emanating from Circular Holes

C.R. Pickthall

DISTRIBUTION

AUSTRALIA

DEFENCE ORGANISATION

Defence Science and Technology Organisation

Chief Defence Scientist
FAS Science Policy
AS Science Corporate Management
} shared copy
Counsellor Defence Science, London (Doc Data Sheet only)
Counsellor Defence Science, Washington (Doc Data Sheet only)
Senior Defence Scientific Adviser (Doc Data Sheet only)
Scientific Advisor Policy and Command (Doc Data Sheet only)
Navy Scientific Adviser (3 copies Doc Data Sheet only)
Scientific Adviser - Army (Doc Data Sheet only)
Air Force Scientific Adviser
Scientific Adviser to Thailand MRD (Doc Data sheet only)
Scientific Adviser to the DRC (Kuala Lumpur) (Doc Data sheet only)

Aeronautical and Maritime Research Laboratory
Director
Library Fishermens Bend
Library Maribyrnong
Chief Airframes and Engines Division
Author: C.R. Pickthall
L.F.R. Rose
A.A. Baker
R. Chester
M. Heller

Electronics and Surveillance Research Laboratory
Director
Main Library DSTOS

Defence Central

OIC TRS, Defence Central Library
Document Exchange Centre, DSTIC (8 copies)
Defence Intelligence Organisation
Library, Defence Signals Directorate (Doc Data Sheet Only)

Navy

Director Aircraft Engineering - Navy
Director of Naval Architecture

Army

Engineering Development Establishment Library
US Army Research, Development and Standardisation Group (3 copies)

Air Force

Aircraft Research and Development Unit
Tech Reports,CO Engineering Squadron,ARDU
CLSA-LC
DTA AS1-LC
OIC ATF, ATS, RAAFSTT, WAGGA (2 copies)

UNIVERSITIES AND COLLEGES

Australian Defence Force Academy
Library
Head of Aerospace and Mechanical Engineering

Flinders
Library

LaTrobe
Library

Melbourne
Engineering Library

Monash
Hargrave Library

Newcastle
Library
Institute of Aviation

New England
Library

Sydney
Engineering Library

NSW
Physical Sciences Library

Queensland
Library

Tasmania
Engineering Library

Western Australia
Library

RMIT
Library

University College of the Northern Territory
Library

OTHER GOVERNMENT DEPARTMENTS AND AGENCIES

AGPS

OTHER ORGANISATIONS

NASA (Canberra)
BHP, Melbourne Research Laboratories

SPARES (7 COPIES)

TOTAL (60 COPIES)

AL 149 DEPARTMENT OF DEFENCE

PAGE CLASSIFICATION
UNCLASSIFIED

DOCUMENT CONTROL DATA

—
PRIVACY MARKING

1a. AR NUMBER	1b. ESTABLISHMENT NUMBER	2. DOCUMENT DATE	3. TASK NUMBER
AR-008-408	DSTO-RR-0005	JULY 1994	AIR 92/089

4. TITLE
Stress Intensity Factors and Crack Mouth Openings for Bridged Cracks Emanating from Circular Holes

5. SECURITY CLASSIFICATION (PLACE APPROPRIATE CLASSIFICATION IN BOX(S) IE. SECRET (S), CONF. (C) RESTRICTED (R), LIMITED (L), UNCLASSIFIED (U)).

DOCUMENT	TITLE	ABSTRACT
U	U	U

6. NO. PAGES
64

7. NO. REFS.
5

8. AUTHOR(S)
C.R. Pickthall

9. DOWNGRADING/DELIMITING INSTRUCTIONS
Not applicable.

10. CORPORATE AUTHOR AND ADDRESS

AERONAUTICAL AND MARITIME RESEARCH LABORATORY
AIRFRAMES AND ENGINES DIVISION
GPO BOX 4331
MELBOURNE VIC 3001 AUSTRALIA

11. OFFICE/POSITION RESPONSIBLE FOR:

RAAF DTA-LC

SPONSOR

SECURITY -

DOWNGRADING -

APPROVAL CAED

12. SECONDARY DISTRIBUTION (OF THIS DOCUMENT)
Approved for public release.
OVERSEAS ENQUIRIES OUTSIDE STATED LIMITATIONS SHOULD BE REFERRED THROUGH DSTIC, ADMINISTRATIVE SERVICES BRANCH, DEPARTMENT OF DEFENCE, ANZAC PARK WEST OFFICES, ACT 2601

13a. THIS DOCUMENT MAY BE ANNOUNCED IN CATALOGUES AND AWARENESS SERVICES AVAILABLE TO ....
No limitations.

14. DESCRIPTORS
Cracking (fracturing)
Stress
Fracture tests
Transverse strength
Complex variables
Circles (geometry)

15. DISCAT SUBJECT CATEGORIES

16. ABSTRACT
Muskhelishvili's method of complex potentials has been applied to the problems of one crack, and two diametrically opposed (symmetrical) cracks emanating from a circular hole of radius R, subjected to a biaxial load. The cracks of length a, are orthogonal to the principal applied stress σ^{∞}_{yy}, with transverse stress $\sigma^{\infty}_{xx} = \lambda\sigma^{\infty}_{yy}$. This work extends previous work through the inclusion of linear springs with spring constant k bridging the crack opening. Analysis focussed on the (normalized) design parameters of crack tip stress intensity factor F_n and crack mouth opening V_n. Their dependencies on biaxiality λ, normalized spring stiffness ka, and the geometry specified by $a_n = a/(a + R)$, were investigated. Interpolation formulae with parameters depending on a_n were fitted to the high and low ka limits of F_n and V_n. These provided a simple means for calculating F_n and V_n, in most cases to within a few percent of the numerically calculated values. An interesting comparison of the symmetrically cracked hole to the partially bridged centre crack, showed that the latter had a lower stress intensity factor in all but the very short crack cases.

PAGE CLASSIFICATION
UNCLASSIFIED

PRIVACY MARKING

THIS PAGE IS TO BE USED TO RECORD INFORMATION WHICH IS REQUIRED BY THE ESTABLISHMENT FOR ITS OWN USE BUT WHICH WILL NOT BE ADDED TO THE DISTIS DATA UNLESS SPECIFICALLY REQUESTED.

16. ABSTRACT (CONT).		
17. IMPRINT **AERONAUTICAL AND MARITIME RESEARCH LABORATORY, MELBOURNE**		
18. DOCUMENT SERIES AND NUMBER DSTO Research Report 0005	19. WA NUMBER 36 341B	20. TYPE OF REPORT AND PERIOD COVERED
21. COMPUTER PROGRAMS USED		
22. ESTABLISHMENT FILE REF.(S)		